SEQUENCE-STRATIGRAPHIC ARCHITECURE AND FACIES OF THE MIDDLE TO UPPER JURASSIC PREUSS AND STUMP FORMATIONS

by

RICHARD HESS

(Under the Direction of Steven M. Holland)

ABSTRACT

Few studies specifically test the principles of sequence stratigraphy in foreland basins, where rates of accommodation and sedimentation increase from the distal portions of the basin into the foredeep. The Middle to Upper Jurassic Preuss and Stump formations of the Wyoming Range, Wyoming and Idaho, were deposited in the foredeep of the Sundance Seaway, and a facies and sequence-stratigraphic analysis was undertaken to understand how the sequence architecture of the foredeep correlates to the previously established architecture of the Jurassic strata in the Bighorn Basin. The Middle to Upper Jurassic strata of the foredeep consist of one partially complete depositional sequence and this sequence is equivalent to the J-4 sequence in the Bighorn Basin. The sequence architecture of the foredeep suggests that tectonic subsidence and the position of the shoreline in the high or low-accommodation zone play a primary control on the sequence architecture of a foreland basin.

INDEX WORDS: siliciclastic rocks; Jurassic; foreland basin; sequence stratigraphy

SEQUENCE-STRATIGRAPHIC ARCHITECURE AND FACIES OF THE MIDDLE TO UPPER JURASSIC PREUSS AND STUMP FORMATIONS

by

RICHARD HESS

B.A., Colorado College, 2016

A Thesis Submitted to the Graduate Faculty of The University of Georgia in Partial Fulfillment of the Requirements for the Degree

MASTER OF SCIENCE

ATHENS, GEORGIA

2019

SEQUENCE-STRATIGRAPHIC ARCHITECURE AND FACIES OF THE MIDDLE TO UPPER JURASSIC PREUSS AND STUMP FORMATIONS

by

RICHARD HESS

Major Professor:	Steven M. Holland
Committee:	David S. Leigh
	Clark R. Alexander

Electronic Version Approved:

Suzanne Barbour
Dean of the Graduate School
The University of Georgia
August 2019

DEDICATION

I would like to dedicate this thesis to my grandfather Ruben Ross whose paleontological and geological pursuits first inspired my interest in the geosciences. His influence was the primary reason I took my first geology course at Colorado College. I continue to be inspired by him and his work on a daily basis.

ACKNOWLEDGEMENTS

Thank you to Steve Holland for being an amazing advisor whose insight and guidance made this project possible. I am grateful also to Clark Alexander and David Leigh for serving on my committee. Thank you also to Skip Sliester and Pedro Monarrez for assistance in the field. Many thanks to Sierra Swenson, Pedro Monarrez, Garett Brown, Sarah Wright, and Bolton Howes for their advice, conversations, and support throughout this project.

Thank you to the Miriam Watts-Wheeler fund, the Gilles and Bernadette Allard Fund, and the Tobacco Root Geological Society Field Scholarship for their generous funding of this project.

My thanks as well to my family (Richard, Alison, and Annie) and Sierra for their love and support.

TABLE OF CONTENTS

Page

LIST OF TABLES

Page

LIST OF FIGURES

Page

CHAPTER 1

INTRODUCTION AND LITERATURE REVIEW

This thesis has been prepared as a manuscript intended for submission to the *Journal of Sedimentary Research*. The second chapter includes the manuscript, with an introduction, geologic setting, conceptual background, methods, facies association, sequence-stratigraphic interpretation, discussion, and conclusion. The third chapter summarizes conclusions. This project develops three distinct facies models for the Giraffe Creek Member of the Twin Creek Formation, The Preuss Formation, and the Stump Formation, describes the sequence-stratigraphic architecture of the foredeep of the Sundance Seaway during the Middle to Upper Jurassic, and correlates the stratigraphic architecture of the Middle to Upper Jurassic strata in the foredeep to the previously established sequence-stratigraphic architecture of distal portions of the Sundance Seaway in the Bighorn Basin.

The application of sequence-stratigraphic concepts in foreland basins is well documented (e.g. Van Wagoner and Bertram 1995). Foreland basins have a wide variation in rates of sedimentation and subsidence (Posamentier and Allen 1993). Because variations in subsidence affect accommodation and the resulting depositional sequences, one study proposed a theoretical framework of sequence stratigraphy in foreland basins (Posamentier and Allen 1993). To understand how changes in relative sea level affect the sequence-stratigraphic architecture of a foreland basin, the basin was divided into high and low-accommodation zones. It was proposed that tectonic

subsidence and the location of the shoreline within these zones would be the primary control on the sequence-stratigraphic architecture of a foreland basin (Posamentier and Allen 1993). Understanding the sequence-stratigraphic architecture of a foreland basin is important because it tests the principles of sequence stratigraphy, where rates of accommodation and sedimentation increase from the distal portions of the basin into the foredeep. The Sundance Seaway is a good setting to test the principles of sequence stratigraphy because the architecture of the distal portion of the basin is well-established in the Bighorn Basin (McMullen at al. 2014; Clement and Holland 2016; Danise and Holland 2018).

The Preuss and Stump formations are interpreted to have been deposited in the foredeep because of a significant westward thickening of the formations, the Preuss is over 17 times thicker in Idaho than in southwestern Wyoming (Hileman 1973; Pipiringos and Imlay 1979). The Preuss and Stump formations have had little study, and most of it has been lithostratigraphic (Imlay 1952, 1980, Pipiringos and Imlay 1979). Pipiringos and O'Sullivan (1978) conducted a study on the regional unconformities of the Mesozoic, but it predates the application of sequence-stratigraphic principles to correlation. Cook (2016) conducted one unpublished study on the sequence-stratigraphic architecture of the Preuss Formation in Utah, Wyoming, and Idaho. Wilcox and Currie (2008) conducted a study on the sequence-stratigraphic architecture of the Stump Formation in northwestern Utah.

CHAPTER 2

THE SEQUENCE-STRATIGRAPHIC ARCHITECTURE AND FACIES OF THE MIDDLE TO UPPER JURASSIC PREUSS AND STUMP FORMATIONS[1]

[1] Hess, R.M. and S.M. Holland. To be submitted to *Journal of Sedimentary Research.*

ABSTRACT

The application of sequence-stratigraphic concepts to foreland basins is well documented. Few studies specifically test the principles of sequence stratigraphy in foreland basins, where rates of accommodation and sedimentation increase from the distal portions of the basin into the foredeep. The Middle to Upper Jurassic Preuss and Stump formations of the Wyoming Range, Wyoming and Idaho, USA, were deposited in the foredeep of the Sundance Seaway, and a facies and sequence-stratigraphic analysis was undertaken to understand how the sequence architecture of the foredeep correlates to the previously established architecture of Middle and Upper Jurassic strata in the Bighorn Basin. The Giraffe Creek Member of the Twin Creek Formation, the Preuss Formation, and Stump Formation record three distinct facies associations. The Giraffe Creek Member was deposited on a carbonate ramp, the Preuss Formation was deposited on a siliciclastic tidally dominated coast, and the Stump Formation was deposited on a low-energy, wave-dominated shelf. The Giraffe Creek Member, the Preuss Formation, and the Stump Formation represent one partially complete depositional sequence. This depositional sequence is equivalent to the J-4 sequence in the Bighorn Basin as described by McMullen et al. (2014) and Danise and Holland (2018). The lowstand systems tract is equivalent to the J-4 unconformity updip in the distal portion of the basin. The transgressive and highstand systems tracts are equivalent to the Redwater Shale and Windy Hill Members of the Sundance Formation. The results of this study provide support for the theoretical framework for foreland basin sequence stratigraphy proposed by Posamentier and Allen (1993). The sequence architecture of the foredeep suggests that the rate of tectonic subsidence and the position of the shoreline in the high or low-

accommodation zone are the primary controls on the sequence architecture of a foreland basin.

INTRODUCTION

The principles of sequence stratigraphy were initially developed based on stratal relationships observed on passive continental margins (Vail et al. 1977, 1984). Because passive continental margins had been thought to be relatively unaffected by tectonics, it was likely the initial model of sequence stratigraphy would need to be modified when applied to tectonically active sedimentary basins like foreland basins. Unlike a passive margin, foreland basins have a wide variation in both sedimentation and subsidence rates (Posamentier and Allen 1993; DeCelles and Giles 1996). This creates two questions: do the principles of sequence stratigraphy need to be modified in a foreland basin in response to variations in subsidence, and what is the sequence-stratigraphic architecture of a foreland basin?

Since then, much work has been done on the sequence stratigraphy of foreland basins (e.g., Van Wagoner et al. 1990; Elrick and Read 1991; Mellere 1994; Aitken and Flint 1995; Van Wagoner 1995). One particular study argued that the sequence-stratigraphic model did need to be modified in a foreland basin, and it provided a theoretical framework to understand their depositional sequences (Posamentier and Allen 1993). Although sequence-stratigraphic concepts have been applied to foreland basins (e.g. Van Wagoner and Bertram 1995), apparently no field studies specifically test the conceptual framework of Posamentier and Allen (1993) of how sequence-stratigraphic architecture varies across a foreland basin. This study aims to test that framework by answering two specific questions. First, what is the sequence-stratigraphic architecture of

the foredeep, the region of greatest subsidence in a foreland basin? Second, how does the architecture of the foredeep relate to the distal portion of a foreland basin, which subsides more slowly? Answering these questions will test the principles of sequence stratigraphy as accommodation and sediment supply increase from the distal portions of the basin into the foredeep.

The Jurassic Sundance Seaway of the western United States is an ideal setting to test the work of Posamentier and Allen (1993), as the sequence-stratigraphic architecture of the distal portions of the basin are well understood (McMullen et al. 2014; Clement and Holland 2016; Danise and Holland 2018). The Middle and Upper Jurassic marine rocks of the Sundance Seaway, the Sundance and Gypsum Spring formations of central Wyoming, contain seven third-order (i.e., 1–10 m.y. duration) depositional sequences (McMullen et al. 2014; Clement and Holland 2016; Danise and Holland 2017). Although the sequence-stratigraphic architecture along the distal portion of this retroarc foreland basin is well-established, the architecture is unknown in the foredeep to the west along the Wyoming–Idaho border. There, the Middle to Upper Jurassic Preuss Formation, a red mudstone–sandstone unit, and the Stump Formation, a tan to buff shale–sandstone unit, are exposed throughout the Wyoming–Idaho fold and thrust belt (Imlay 1952; Hileman 1973; Pipiringos and O'Sullivan 1978; Pipiringos and Imlay, 1979). The Preuss and Stump are interpreted to lie within the foredeep because of the significant westward thickening of the formations: the Preuss Formation is 400 m thick in parts of Idaho, thirteen times thicker than equivalent rocks in central Wyoming (Hileman 1973; Pipiringos and Imlay 1979). Building on the previously established sequence-stratigraphic architecture of the Sundance Seaway (McMullen et al. 2014; Clement and

Holland 2016; Danise and Holland 2017), this study examines the sequence-stratigraphic architecture of the Preuss and Stump formations and how their architecture relates to the distal, more slowly subsiding portions of the foreland basin.

GEOLOGIC SETTING

The Preuss and Stump formations are exposed in western Wyoming, eastern Idaho, and northern Utah (Imlay 1952; Hileman 1973; Pipiringos and Imlay 1979; Wilcox and Currie 2008). The Preuss and Stump formations were deposited in the Sundance Seaway, a retroarc foreland basin with a volcanic arc and fold and thrust belt to the west and the North American craton to the east (Bjerrum and Dorsey 1995; Fig. 1). The Sundance Seaway occupied this foreland basin, and the seaway extended from southern Utah to British Colombia. The position of the entrance to the seaway is uncertain, but it may have been as far north as the southern Yukon Territory (Schuchert 1923, Parcell and Williams 2005; Blakey 2015), or as far south as the United States–Canada border (Frebold et al. 1958; Imlay 1980). Estimates of paleolatitude of southwest Wyoming during the Bajocian and Bathonian vary from 22–25^{o} N (Kocurek and Dott 1983) to 35–38^{o} (Blakey 2015), consistent with a subtropical to temperate latitude.

The Jurassic formations of the western United States contain five regional unconformities (Pipiringos and O'Sullivan 1978). The formational contacts and position of these unconformities within the Stump and Preuss formations have been the focus of several studies (Imlay 1952; Hileman 1973; Pipiringos and Imlay 1979). The Preuss Formation unconformably (J-2 unconformity) overlies the Giraffe Creek Member of the Twin Creek Limestone (Imlay 1952; Hileman 1973). The Curtis Member of the Stump Formation is bounded below and above by unconformities, the J-3 and J-4

unconformities. The J-3 unconformity at its base lies at its contact with the Preuss Formation. The J-4 unconformity lies at its upper contact with the Redwater Member of the Stump Formation. The nature of the unconformity between the Preuss Formation and overlying Stump Formation is unclear, even disputed. Although some interpret the contact of the Preuss and Stump formations as unconformable (Imlay 1952), others have argued that it is conformable (Hileman 1973; Pipiringos and Imlay 1979). The nature of the contact between the Stump and the overlying Morrison Formation is unclear as well. The contact is unconformable (J-5 unconformity) in the Uinta Mountains (Wilcox and Currie 2008), but at Lower Slide Lake, just east of the Teton Mountains, the contact appears to be conformable (Hileman 1973).

The Preuss Formation has had little study, most of it lithostratigraphic (Imlay 1952, 1980; Hileman 1973; Pipiringos and Imlay 1979). These studies report alternating beds of unfossiliferous red mudstone and sandstone. Gypsum nodules and silica concretions are found throughout the Preuss in Wyoming and Idaho. In Idaho, the lower Preuss contains halite beds that can be more than 20 m thick, and fossiliferous limestones are present. This limestone unit contain pelecypods, gastropods, corals, oysters, and crinoid columnals (Imlay 1952; Hileman 1973). Fossils are found only in the limestone, and the Preuss is usually unfossiliferous. The Preuss has been interpreted to represent marine and marginal marine depositional environments (Imlay 1952; Hileman 1973; Cook 2016). Only one sequence-stratigraphic study on the Preuss Formation has been attempted (Cook 2016), and it described five different facies within the formation: an open marine facies, a restricted marine facies, a coastal sabkha facies, an inland sabkha facies, and an alluvial facies (Cook 2016). This unpublished study also reported second-

order sequence boundaries (a second-order sequence has a duration of 10–100 m.y.) at the base and top of the Preuss and three third-order sequence boundaries within the Preuss.

Although the precise age of the Preuss Formation is poorly constrained, it is thought to be Callovian because of its unconformable lower contact with the Callovian Giraffe Creek Member and its unconformable contact with the overlying Stump Formation (Imlay, 1952, 1980, 1982; Hileman, 1973; Pipiringos and Imlay 1979; Fig. 2). The Stump Formation is considered to be Oxfordian because of the presence of the ammonite *Cardioceras hyatti*, which correlates to the *Cardioceras cordatum* ammonite zone (Imlay 1952, 1980, 1982; Pipiringos and Imlay 1979; Fig. 2).

Most studies of the Stump Formation have been lithostratigraphic as well (Imlay 1952, 1980; Hileman 1973; Pipiringos and Imlay 1979). The Stump Formation consists of three main divisions, a lower sandstone, a middle shale, and an upper sandstone (Pipiringos and Imlay 1979). The lower sandstone is always assigned to the Curtis Member, and the upper sandstone unit is always assigned to the Redwater Shale Member. The middle shale unit is sometimes assigned to the upper Curtis Member (Fig. 4 in Pipiringos and Imlay 1979), sometimes the lower Redwater Shale Member (Fig. 7 in Pipiringos and Imlay 1979), and sometimes both (Fig. 5, locality 4 in Pipiringos and Imlay 1979). The Stump Formation is more fossiliferous than the Preuss, but it is still relatively unfossiliferous. The Stump is reported to contain oysters, ammonites, brachiopods, mussels, scallops, belemnites, decapods, pelecypods, ichthyosaurs, pliosaurs, as well as dinosaur and pterosaur tracks (Hileman 1973; Pipiringos and Imlay 1979; Bilbey et al. 1990, 2005; Chure 1993; Feldmann and Titus 2006). Only one

sequence-stratigraphic analysis of the Stump Formation has been attempted (Wilcox and Currie 2008), and it interpreted the Stump as being wave-dominated and deposited during the transgressive and highstand systems tract of a single unconformity-bounded sequence.

CONCEPTUAL BACKGROUND

To understand how the sequence-stratigraphic architecture of foreland basins differs from that of passive margins, it is important to understand which tectonically controlled parameters affect stratal patterns. Modern examples of foreland basins include the Persian Gulf and the Po Basin of Italy, and modern examples of passive margins include the eastern coasts of North and South America. During a eustatic sea-level cycle, stratal patterns are controlled by two tectonic factors: temporal variations in the rate of subsidence or uplift, and spatial variations in this rate (Posamentier and Allen 1993). On passive margins, subsidence rates increase seaward away from the craton, but in contrast, subsidence rates in foreland basins decrease away from the orogenic belt towards the craton (Posamentier and Allen 1993; DeCelles and Giles 1996; Fig. 3).

The structure of a foreland basin results from the spatially variable subsidence trend seen within the basin. A foreland basin is bounded on one side by an orogenic belt and the continental craton on the other (DeCelles and Giles 1996). The basin can be divided into four primary zones of deposition: the wedge top, the foredeep, the forebulge, and the back-bulge basin (Fig. 4). In a foreland basin, subsidence is driven by flexural loading of the orogenic belt and the wedge-top depozone (Fig. 4; DeCelles and Giles 1996). The width and depth of the basin, the location of the forebulge, and the rates of subsidence are controlled by the rigidity of the lithosphere and the mass of the orogenic

load (Beaumont et al. 1988; Pope et al. 2009). For example, if the rigidity of the lithosphere underlying a foreland basin were to decrease but the orogenic load remained constant, subsidence rates would increase throughout the basin, and the basin would become narrower. In contrast, if the lithospheric rigidity is held constant and the orogenic load is increased, the basin would deepen, but the width would not change.

Generally, the rigidity of the lithosphere is thought to be roughly constant across a foreland basin and through time, with the size of orogenic load varying through time (DeCelles and Giles 1996). Therefore, temporal variations in subsidence rate within a foreland basin system are driven by flexural responses to changes in the orogenic load. In foreland basins, the orogenic belt is built by thrusting. Because thrusting occurs episodically, the orogenic load and the subsidence rate vary through geologic time (Posamentier and Allen 1993; DeCelles and Giles 1996). When thrusting is active, the total orogenic load increases, which increases subsidence rates. During episodes of tectonic quiescence with no thrusting, the orogenic load erodes, causing uplift in the basin.

Because variable subsidence rates in a foreland basin affect relative sea level (i.e., accommodation) and the resulting depositional sequences, a theoretical framework of sequence stratigraphy for foreland basins has been proposed (Posamentier and Allen 1993). To simplify how changes in relative sea level affect stratal patterns in a foreland basin, a basin can be divided into high-accommodation and low-accommodation zones (Fig. 3), which are defined by the position of the point at which the maximum rate of eustatic sea-level fall equals the rate of subsidence within the basin. During a eustatic sea-level cycle, a subaerial unconformity cannot form in the high-accommodation zone

because the rate of subsidence exceeds the rate of fall in eustatic sea level. An unconformity will form in the low-accommodation zone when the rate of eustatic sea-level fall exceeds the rate of subsidence.

The location of the shoreline in the high or low-accommodation zone during a eustatic sea-level cycle will determine the architecture of depositional sequences formed in a foreland basin. If the shoreline is in the high-accommodation zone, no relative fall in sea level will occur, creating depositional sequences without sequence-bounding unconformities (i.e. Type 2 Sequences) to develop (Fig. 5). These sequences are defined by progradation and aggradation of the shore during the shelf-margin systems tract (SMST), followed by retrogradational stacking in the transgressive systems tract (TST), followed by renewed progradation in the highstand systems tract (HST). Because no subaerial unconformity forms within the high-accommodation zone, the highstand systems tract of the underlying sequence and the shelf-margin systems tract are difficult or impossible to distinguish. If the shoreline is located in the low-accommodation zone, type 1 depositional sequences will develop (i.e., sequences bounded by an unconformity). A type 1 depositional sequence begins with the seaward and downward displacement of the shore coupled with the updip formation of an unconformity, followed by slow progradation and aggradation (LST), capped by retrogradational stacking and transgression of the shoreline (TST), and finally by renewed progradation in the highstand systems tract (HST). The area of the shelf exposed during the initial period of relative sea-level fall becomes a zone of sedimentary bypass, creating a subaerial unconformity and causing sediment to be deposited on basinally isolated shorelines.

In foreland basin systems, differing stratigraphic architectures will develop in the distal (edge of the foredeep and forebulge; Fig. 4) and proximal (foredeep) portions of the basin. The distal portion of the basin always lies within the low-accommodation zone. During a eustatic sea-level cycle, subsidence will likely be less than the rate of eustatic sea-level fall, causing a relative fall in sea level and forming a subaerial unconformity in the distal portion of the basin (i.e., Type 1 Sequence). In contrast, the proximal portion of the basin is located within the high-accommodation zone at least during times of active thrusting. During a eustatic sea-level cycle, subsidence will likely be greater than the rate of eustatic sea-level fall, and a relative sea-level fall will therefore not occur in the proximal portion of the basin (i.e., Type 2 sequence). The differences in the rate of subsidence across a foreland basin allow the expected systems tracts in the proximal and distal portions of the basin to be predicted (Fig. 5). In the proximal portion of the basin, shelf-margin systems tract (SMST), and transgressive systems tract (TST), and highstand systems tract (HST) would be expected. In the distal portion of the basin the lowstand systems tract (LST), transgressive systems tract (TST), highstand systems tract (HST), and falling-stage systems tract (FSST) would be expected.

METHODS

Seven stratigraphic sections of the Stump and Preuss Formation were measured across the Wyoming Range in southwest Wyoming (Fig. 6; Appendix A; Appendix B). At each section, lithology, sedimentary structures, body fossils, and trace fossils were documented. Twenty-four hand samples were thin-sectioned along stratigraphic position when possible and stained for facies analysis. Nine geophysical logs from boreholes were obtained from the Wyoming Oil and Gas Conservation Commission (Wyoming Oil and

Gas Conservation Commission 2018). Comparison of well logs to nearby outcrops was used to establish the interpretation of the well-log signatures. The well logs and two columns are organized along two cross sections (Fig. 6). The south to north transect (A to A′) reflects the direction of long term progradation (Wilcox and Currie 2008; Blakey 2015). The east to west transect (B to B′) reflects a high to low subsidence gradient (Bjerrum and Dorsey 1995; Danise and Holland 2018). The wells were used to correlate the Stump and Preuss formations in the subsurface throughout the Wyoming Range. Backstripping of the La Barge Creek column from this study and Howes (2017) was used to reconstruct the timing and magnitude of relative sea-level changes during the deposition of the Twin Creek Limestone, Preuss Formation, and Stump Formation. Backstripping solves the accommodation space equation using sediment thickness and estimates of water depth. Estimates of sediment thickness are from measured sections and estimates of water depth are based on facies interpretations. The backstripping analysis used an Airy backstripping routine to correct for compaction and isostatic loading (Watts 1988; Sahagian and Holland 1991). Backstripping was performed using the macOS application Backstrip (Hunt Mountain Software 2017).

FACIES

The Giraffe Creek Member of the Twin Creek Limestone, the Preuss Formation, and the Stump Formation each have a unique set of facies reflecting differing suites of depositional environments. Each facies is characterized by a distinctive set of lithologies, bedding, sedimentary structures, fossils, and facies contacts (Tables 1–3). Seven facies are present in the Giraffe Creek Member, five facies are present in the Preuss Formation, and four facies are present in the Stump Formation. The facies of the Giraffe Creek

Member are interpreted to represent a series of environments along a carbonate ramp including foreshoal, ooid shoal, backshoal, lagoonal, peritidal flat, and silt flat (Table 1). One facies is interpreted as a sabkha. The facies of the Preuss Formation are interpreted to represent a series of environments along a siliciclastic tidally-dominated coast including sand flat, mixed flat, and mud flat (Table 2). Two facies are interpreted to represent floodplain and fluvial channel. The facies of the Stump Formation are interpreted to represent a series of environments along a siliciclastic wave-dominated shelf including offshore–offshore transition, shoreface, and foreshore (Table 3).

Carbonate Ramp Facies

Facies Gc1: Heterolithic Skeletal Ooid Grainstone.—The abundance of very thin beds of ooids interbedded with planar-laminated lime mudstone, and the abundance of vortex ripples and small-scale trough cross stratification suggest deposition adjacent to an ooid sand body such as a beach, tidal delta, or shoal (Simone 1980; Burchette et al., 1990). The lack of bioturbation and vertical thickening of ooid beds is consistent with deposition increasingly proximal to an ooid shoal (Elrick and Read, 1991; Smith and Read 2001). Facies Gc1 grades upwards into Facies Gc2, a medium-bedded ooid grainstone, suggesting deposition in the foreshoal. Facies Gc1 is the deepest water facies in this association.

Facies Gc2: Ooid Grainstone.— The abundance of very thin-bedded to medium-bedded skeletal ooid grainstone, with large-scale trough cross stratification and a lack of bioturbation suggests that Facies Gc2 was deposited in an ooid shoal (Fig. 7; Elrick and Read 1991; Smith and Read 2001). The presence of lime mudstone intraclasts and shell lags at set boundaries could be the result of two different processes: 1) periodic storms

that winnowed away fine-grained sediments, or 2) as lags in intrashoal channels. The former is more likely given the relative lateral discontinuity of the shell beds, no more than a 0.5–1 m in length. If the shell lags and mudstone intraclasts were deposited in intrashoal channels, these beds would be thicker and more laterally continuous. Facies Gc2 gradationally overlies facies Gc1 and fines upwards into Facies Gc3.

Facies Gc3: Heterolithic Carbonate Mudstone.— The abundance of thin, planar-laminated beds of lime mudstone interbedded with very thin lenticular beds of ooid grainstone, and the presence of small-scale cross stratification, vortex ripples, and locally megaripples suggest deposition peripherally to an ooid sand body such as on a beach, tidal delta, or shoal (Simone 1980; Burchette et al., 1990). The lack of bioturbation and vertical thinning of ooid beds is consistent with deposition distal to an ooid shoal (Elrick and Read, 1991; Smith and Read 2001). Facies Gc3 gradationally overlies Facies Gc2 and grades upwards into Facies Gc4, suggesting deposition in the backshoal.

Facies Gc4: Planar-laminated Lime Mudstone.— The abundance of lime mud, lack of fossils, planar lamination, and stratigraphic relationship to Facies Gc3 suggests that Facies Gc4 was deposited in a restricted shallow-subtidal setting (Clement and Holland 2016). Facies Gc4 gradationally overlies facies Gc3 and is increasingly planar-laminated upwards. The presence of planar lamination and the very thin bedding indicates minimal bioturbation (Droser and Bottjer 1993). A lack of bioturbation is consistent with elevated salinity, suggesting restricted conditions, as salinity can be a primary control on the

degree of bioturbation (Ekdale 1988). Facies Gc4 gradationally overlies Facies Gc3 and grades upwards into Facies Gc5, suggesting deposition in a lagoonal setting.

Facies Gc5: Dolomitic Lime Mudstone.— Based on the abundance of dolostone, the presence of microbial laminae, and the gradational lower contact with Facies Gc4, Facies Gc5 is interpreted to have been deposited in a peritidal setting (Bachmann and Hirsch 2006; Flügel 2010). The sedimentary structures in Facies Gc5 also provide evidence for an intertidal environment (Fig. 7). Desiccation cracks form as a result of subaerial exposure during low tide (Plummer and Gostin 1981; Bachmann and Hirsch 2006; Noffke et al. 2006). It is possible that some of the desiccation cracks viewed in cross section may be synaeresis cracks, which would also be consistent with an intertidal interpretation, as they form subaqueously from rapid changes in salinity (Plummer and Gostin 1981). Facies Gc5 gradationally overlies Facies Gc4 and grades upwards into Facies Gc6, suggesting deposition on a tidal flat.

Facies Gc6: Red Siltstone.— The dominance of red to brown siltstone, the absence of body or trace fossils, and the gradational underlying contact with Facies Gc5 suggests that Facies Gc6 was deposited on a supratidal mud flat (Fig. 7; Evans et al. 1969; Clement and Holland 2016). Ferric iron is the presumed cause of the reddish-brown color of the sediment, indicating deposition in an oxic setting, which suggests flushing by oxygen-rich meteoric water or low organic carbon input (Maynard 1982). The red to brown color is similar to the desert mud flat facies seen farther to the east in the Sundance Seaway in central Wyoming and southern Montana (Parcell and Williams 2005; Clement and Holland 2016; Danise and Holland 2018). Facies Gc6 gradationally overlies Facies Gc5, indicating that these facies were adjacent. Facies Gc6 is always

overlain by a flooding surface, suggesting that it is the most landward or depositionally up-dip facies in this association.

Facies Gc7: Gypsum Rich Red Siltstone.—The dominance of red to brown siltstone, the absence of body or trace fossils, the mosaic (chicken-wire) texture, and the gradational underlying contact with Facies Gc5 suggests that Facies Gc7 was deposited on a sabkha (Warren and Kendall 1985; Kendall 2010). The gradual upward transition from Facies Gc5 and close association with Facies Gc6 suggest that some portions of Facies Gc7 were deposited on mud flats and sabkhas adjacent to a peritidal zone. Facies Gc7 is similar to the sabkha facies reported from the Sundance Seaway in central Wyoming and southern Montana (Parcell and Williams 2005; Clement and Holland 2016; Danise and Holland 2018). Facies Gc7 is seen only on the westernmost thrust sheets in this study.

Facies Model.— The vertical and lateral facies relationships of the Giraffe Creek Member of the Twin Creek Limestone indicate that deposition took place on the inner portion of a carbonate ramp (Fig. 8). Gradual vertical transitions among facies indicate laterally adjacent depositional environments. Gradual facies transitions are represented by a gradual change in lithology from dolomitic lime mudstone (Gc5) to red siltstone (Gc6), or through the intertonguing of facies, with one facies progressively dominating over another, such as the vertical transition from ooid grainstone (Gc2) to heterolithic lime mudstone (Gc3).

Six of the seven facies present in the Giraffe Creek Member of the Twin Creek Limestone have repeated gradual transitions that reveal the spatial arrangement of the depositional environments on the ramp. Facies Gc1 (heterolithic skeletal ooid grainstone)

is the most basinward facies, and it is interpreted to have been deposited in a foreshoal setting. Facies Gc1 grades upwards into Facies Gc2 (ooid grainstone), interpreted as recording deposition in an ooid shoal. Facies Gc2 grades upwards into Facies Gc3 (heterolithic lime mudstone), interpreted as a backshoal setting. Facies Gc3 grades upwards into Facies Gc4 (planar-laminated lime mudstone), interpreted as recording deposition in a lagoonal setting. Facies Gc4 grades upwards into Facies Gc5 (dolomitic lime mudstone) interpreted as peritidal flats. Facies Gc5 grades upwards into Facies Gc6 (red mudstone), interpreted to have been a desert mudflat, the most landward environment in this facies association. Facies Gc5 grades upwards into Facies Gc7 (gypsum-rich, red siltstone), interpreted as a sabkha. Because Facies Gc7 occurs only at the Cabin Creek locality, the lateral extent of sabkha facies during Giraffe Creek deposition is unknown.

There are many similarities between the facies model for the Giraffe Creek Member of the Twin Creek Limestone and the facies models for coeval strata in the Bighorn Basin and southwestern Wyoming (Parcell and Williams 2005; McMullen et al. 2014; Clement and Holland 2016; Danise and Holland 2018). The facies model from Parcell and Williams (2005) has equivalents to Facies Gc2 (their Facies IV), Gc4 (III), Gc6 (I), and Gc7 (II), with similar environmental interpretations. Parcell and Williams (2005) recognized a deeper-water carbonate mudstone facies not seen in the Giraffe Creek, suggesting that their study extended to a deeper water setting. This is expected, given their study area is to the north of the present study area. Clement and Holland (2016) recognize equivalents to Facies Gc2 (their Facies OG), Gc4 (LLM), Gc5 (DM), Gc6 (RM), and Gc7 (G), with similar environmental interpretations. Clement and

Holland (2016) also describe a paleosol (their Facies PM) not present in the Giraffe Creek. Similarly, trough cross-bedded oolitic facies are present in the Bighorn Basin and southeastern Montana (McMullen et al. 2014). The facies model of Danise and Holland (2018) also has equivalents to Facies Gc2 (their Facies C2), Gc4 (C3), Gc5 (C4), Gc6 (D2a), and Gc7 (D2b), with similar environmental interpretations. Danise and Holland (2018) also recognize eolian dunes (their D5a and C5), which were not recognized in the Giraffe Creek.

The facies model presented here is similar in many ways to other carbonate-ramp facies models (e.g., Burchette and Wright 1992), particularly the inner ramp portion (Facies Gc4–Gc7). For example, the facies model of the Giraffe Creek Member of the Twin Creek Limestone is similar to a carbonate ramp from the Jurassic of the Caspian Basin in Northern Iran (Aghaei et al. 2013), particularly the inner-ramp settings. Like the Giraffe Creek Member, this Iranian Jurassic ramp had ooid shoals that passed landward into lagoonal and tidal flat facies with planar-laminated dolostone. The Iranian ramp differs from the Giraffe Creek ramp in that it lacks sabkha or desert mudflat facies, and it is much more fossiliferous and contains a better developed infauna. The minimal fossils and lack of bioturbation in the Giraffe Creek Member may reflect the elevated salinity and temperatures postulated for the Sundance Seaway (McMullen et al. 2014; Clement and Holland 2016; Danise and Holland 2017, 2018).

Siliciclastic Tidally-Dominated Coast Facies

Pr1: Cross-bedded Sandstone.— The dominance of large-scale cross-stratified fine-grained upward-fining sandstone (Fig. 9), current and wave-generated bedforms, and a gradational upper contact with facies Pr2 suggest Facies Pr1 was deposited on a tidal

sand flat (Dalrymple 2010; Desjardins et al. 2012a). The abundance of climbing ripples suggests rapid deposition on the edges of the sandflat (Dalrymple 2010). The upward fining and vertical increase in bioturbation both support deposition in a tidal sandflat, where shear stress and grain size decrease landwards (Desjardins et al. 2012a). Facies Pr1 grades upwards into Facies Pr2, suggesting that these facies where laterally adjacent. Facies Pr1 is the deepest-water facies in this association.

Pr2: Heterolithic Silty Sandstone.— The abundance of red to brown, silty, very fine sandstone interbedded with very thin beds of mudstone (Fig. 9), flaser and wavy bedding, current and wave-generated bedforms, and gradational underlying contact with Facies Pr1 suggest Facies Pr2 was deposited on the mixed-flat part of a tidal flat (Desjardins et al. 2012a). Facies Pr2 fines upwards with increasing mud content, a trend expected on mixed flats as the depositional system transitions from bedload to suspension fallout (Flemming 2012). The sedimentary structures in Facies Pr2 also provide evidence for an intertidal environment. Desiccation cracks and halite casts are strong indicators of a tidal environment and typically form in shallow-water restricted environments (Gornitz and Schreiber 1981; Plummer and Gostin 1981; Noffke et al. 2006). Ferric iron is the presumed cause of the reddish-brown color of the sediment and indicates deposition in an oxic setting. The reddish-brown color is the result of flushing by oxygen-rich meteoric water or low organic carbon input (Maynard 1982). Facies Pr2 gradationally overlies Facies Pr1 and grades upwards into Facies Pr3, suggesting deposition on a mixed flat.

Pr3: Red Mudstone.— The dominance of red to brown, silty mudstone interbedded with lenticular beds of silty very fine-grained mudstone, and a gradational underlying contact with Pr2 suggests Facies Pr3 was deposited on a mudflat (Desjardins et al. 2012a; Fig. 9).

The reddish-brown color of the sediment indicates deposition in an oxic setting (Maynard 1982). The sedimentary structures in Facies Pr3 also provide evidence for an intertidal environment. Desiccation cracks and halite casts are strong indicators of a tidal environment (Gornitz and Schreiber 1981; Plummer and Gostin 1981; Noffke et al. 2006). Facies Pr3 has a gradational lower contact with Facies Pr2, suggesting deposition in a mudflat. Facies Pr3 is always overlain by a flooding surface and is the most depositionally up-dip facies on the tidal flat.

Pr4: Red Silty Sandstone.— The abundance of red silty sandstone, intense bioturbation, and a gradational upper contact with Facies Pr5 suggest deposition on a floodplain, likely as an overbank deposit (Miall 1977, 1985, 2014). The presence of pedogenic features support deposition in a terrestrial environment. Cutans are pedogenic features that form in the voids in soils (Brewer 1960). They commonly form in arid environments but can also be associated with the rhizosphere (Brewer 1960). The presence of pedogenic features and gypsum nodules suggests these overbank deposits can be classified as either vertisols or gypsisols (Mack and James 1994). Vertisols and gypsisols typically form in dry subtropical climates between the equator and latitudes of 30^{o} (Mack and James 1994). This interpretation is generally consistent with paleolatitude estimates for this area during the Bajocian through Oxfordian (Kocurek and Dott 1983; Blakey 2015; Danise and Holland 2018). Facies Pr4 has a gradational lower contact with Facies Pr5, suggesting deposition on a floodplain. Facies Pr4 is found only on the westernmost thrust sheets in the study area. Facies Pr4 is not found in association with the tidal flat facies (Pr1–Pr3).

Pr5: Erosional Based Sandstone.— The dominance of medium-grained sandstone with an erosional base, basal lag, current-generated bedforms and cross stratification, and a

gradational upper contact with Facies Pr4 suggest Facies Pr5 was deposited in fluvial channels (Appendix B, Preuss Creek; Miall 1977, 1985, 2014). The channels in Facies Pr5 are single-story, suggesting relatively high rates of accommodation (Miall 1985; Miall 2014). Generally, channel thickness is between 1–2 m, suggesting channel depth was shallow. The single erosional base and simple upward-fining architecture of Facies Pr5 suggest deposition in a meandering river; Facies Pr5 does not have the complex architecture that would be produced by multiple channels in a braided river system (Miall 1977, 2014). Facies Pr5 has an erosional base and a gradational upper contact with Facies Pr4, also suggesting deposition in a channel. Facies Pr5 is found only on the westernmost thrust sheets in the study area. Facies Pr5 is not found in association with the tidal flat facies (Pr1–Pr3).

Facies Model.— The vertical and lateral facies relationships of the Preuss Formation indicate deposition took place on a siliciclastic, tidally-dominated coast (Desjardins et al. 2012a; Fig. 10). Gradual vertical transitions among facies indicate laterally adjacent depositional environments. Gradual facies transitions are represented by a gradual change in lithology such as from cross-bedded sandstone (Pr1) to heterolithic silty sandstone (Pr2), or through the gradual intertonguing of facies, with one facies progressively dominating over another, such as the upward transition from heterolithic silty sandstone (Pr2) to red mudstone (Pr3).

Three of the five facies present in the Preuss Formation have repeated gradual transitions that reveal the arrangement of depositional environments on the coast. Facies Pr1 (cross-bedded sandstone) is the most basinward (seaward) facies, and it is interpreted to have been deposited on a sand flat. Facies Pr1 grades upwards into Facies Pr2

(heterolithic silty sandstone), interpreted to have been a mixed flat. Facies Pr2 grades upwards into Facies Pr3 (red mudstone), interpreted to record deposition on a mudflat. Because Facies Pr4 and Pr5 are found only on the westernmost thrust sheets, their lateral relationships to the more basinward facies are unknown. Their occurrence to the west of the tidally influenced facies implies a western sediment source, likely the thrust load in central Idaho (Bjerrum and Dorsey 1995).

There are similarities between the facies model developed for the Preuss Formation and the facies models for coeval strata in northern Utah (Wilcox and Currie 2008) and the Bighorn Basin of central Wyoming (McMullen et al. 2014; Danise and Holland 2018). The Wilcox and Currie (2008) facies model has equivalents to Facies Pr1 (their Sc2b and C4b) and Facies Pr3 (Sc1, C5, and S1), with similar environmental interpretations. Wilcox and Currie (2008) do not have an equivalent to Facies Pr2 because they grouped their mud- and mixed-flat facies together. Wilcox and Currie (2008) also report tidal channels (their facies Sc2a, C1, and C4a) but tidal channels are apparently absent in the exposed portions of the Preuss. McMullen et al. (2014) and Danise and Holland (2018) both have equivalents to facies Pr1 (their Facies T4 and T3) with similar environmental interpretations. McMullen et al. (2014) and Danise and Holland (2018) also report tidal channel and tidal bar facies (their Facies T1, T2, and T3; and T1 and T2). Both studies lack equivalents to Facies Pr2 (mixed flat) and Pr3 (mudflat), suggesting a difference in mud supply between the two coasts. The Preuss tidal coast is notably muddier than the tidally-influenced coasts in the Bighorn Basin (McMullen et al. 2014; Danise and Holland 2018).

The scarcity of tidal channels in the Preuss Formation is intriguing, as tidal channels are found on nearly every modern tidally influenced coast (Hughes 2012). Modern tidal coasts with an absence or poorly developed channels are found on macrotidal coastlines, open-coast tidal flats with a strong wave influence, and coasts that experience freezing or arid conditions for long periods of time (Hughes 2012). In the modern, the high microtidal James Bay at the southern end of Hudson Bay has poorly developed linear tidal channels and tidal flats that lack channels completely. The poorly developed or absent tidal channels in James Bay result from freezing temperatures that stabilize the sediment, covering James Bay with ice up to 6 months out of the year (Hughes 2012). It is possible that the Preuss Formation lacks tidal channels as a result of sediment stabilization (although not from ice, given its paleolatitude), however microbially induced sedimentary structures are absent in the Preuss, making this interpretation unlikely. It is also possible that tidal channels are present in depositionally down dip areas not exposed in the study area. Several well logs down depositional dip from La Barge Creek (logs 49-023-20535, 49-023-20158, and 49-035-20659; Fig. 15) contain sharp-based upward-fining units suggestive of channels. If these upward-fining units are tidal channels, then smaller proximal channels may be present but difficult to distinguish in outcrop at La Barge Creek as a result of their small size, likely on the scale of a bed (~0.5–1 m). In the modern, tidal channels occur seaward from intertidal deposits a similar distance from the tidal channels interpreted in the Preuss Formation. Intertidal flats along the macrotidal eastern coast of Korea can be up to 30 km wide (Alexander et al. 1991). Large tidal channels are interpreted to occur a similar distance from La Barge Creek, approximately 45 km (Fig. 15). This distance may be an even shorter distance

from La Barge Creek because the true position of the shoreline is unknown and the cross-section line may contain a large component of depositional strike.

The facies model developed here for the Preuss Formation bears strong resemblance to other tidally dominated coast facies models (Desjardins et al. 2012a), particularly the tidal flat portion (Facies Pr1, Pr2, and Pr3). For example, on a Cambrian tidal flat deposited on a passive margin in western Canada, fine to medium-grained sandstone deposited on a sandflat passes upwards into heterolithic sandstones in the mixed flat (Desjardins et al. 2012b). This Cambrian tidal flat passes upwards into mudflat environments similar to those in the Preuss Formation. The difference between the Cambrian tidal flat and the Preuss Formation is that the Cambrian tidal flat is more bioturbated and does not contain halite casts, suggesting a more arid setting for the Preuss Formation.

The facies model developed here for the Preuss Formation also resembles the facies models developed for Jurassic tidal flats outside the Sundance Seaway. For example, the Preuss Formation facies model is similar to a tidal flat from the Neuquén Basin in west-central Argentina (McIlroy et al. 2005). Like the Preuss Formation, the tidal flat in the Neuquén Basin has sandflat trough-crossbedded sandstones passing landward into mixed-flat heterolithic sandstone. The mixed-flat facies passes landward into tidal creek and mudflat facies. The Neuquén Basin tidal flat differs from the Preuss Formation in that bioturbation is much more abundant and the presence of detrital organic matter, which is absent in the Preuss Formation, again suggesting a more arid setting for the Preuss.

Siliciclastic Wave-Dominated Shelf Facies

St1: Heterolithic Shale.— The abundance of coarsening-upward thinly laminated shale interbedded with thin beds of sandstone, wave-generated bedforms, and a gradational upper contact with Facies St2, suggest deposition in the offshore transition (Clifton 2006). The abundance of wave-ripple lamination and vortex ripples suggest a low-energy wave-dominated shelf (Clifton 2006). Facies St1 has a gradational upper contact with Facies St2, and it is the deepest water facies in this facies association. Facies St1 is commonly covered throughout the study interval and it is exposed only at McCoy Creek (Appendix B, McCoy Creek).

St2: Amalgamated Sandstone.— The dominance of amalgamated tabular beds of sandstone, bioturbation, and a gradational lower contact with Facies St1 suggests deposition in the lower shoreface (Clifton 2006). The intense bioturbation in the lower shoreface point to deposition in a low-energy coast (Clifton 2006). The *Skolithos* ichnofacies provides additional support for a shoreface interpretation (Pemberton et al. 1992; Fig. 11 D). Facies St2 has a gradational lower contact with Facies St1, and it grades upwards into Facies St3, consistent with deposition in the lower shoreface.

St3: Trough Cross-Stratified Sandstone.— The abundance of sandstone in medium to thin beds, cross stratification, minimal bioturbation, and a gradational lower contact with Facies St2 suggest Facies St3 was deposited in an upper shoreface setting (Clifton 2006; Fig. 11). The presence of large-scale trough cross stratification and a *Skolithos* ichnofacies suggest deposition in the upper shoreface (Pemberton et al. 1992). Shoreface deposits in the Stump Formation typically have a thickness less than 2 m, suggesting a relatively shallow wave base and deposition on a low-energy coast (Howard and Reineck

1981), an interpretation also inferred for shoreface deposits of the Bighorn Basin (McMullen et al. 2014; Danise and Holland 2018). Facies St3 has a gradational lower contact with facies St1, and grades upward into Facies St4, consistent with deposition in an upper shoreface.

St4: Planar-Laminated Sandstone.— The abundance of fine to very fine sandstone, wave-generated bedforms, and a gradational lower contact with Facies St3 suggest Facies St4 was deposited in a foreshore setting (Clifton 2006; Fig. 11). Planar lamination and a lack of bioturbation support deposition in a foreshore environment (Pemberton et al. 1992; Clifton 2006). Facies St4 has a gradational lower contact with St3, also consistent with deposition in the foreshore. Facies St4 is always capped by a flooding surface and is the most depositionally up-dip (landward) facies in this assemblage.

Facies Model.— The vertical and lateral facies relationships of the Stump Formation indicate deposition on a siliciclastic wave-dominated shelf (Fig. 12). Gradual vertical transitions among facies indicate laterally adjacent depositional environments. Gradual facies transitions are represented by a gradual change in lithology such as from trough cross-stratified sandstone (St3) to planar-laminated sandstone (St4), or through the intertonguing of facies, with one facies progressively dominating over another such as the upward transition from heterolithic shale (St1) to amalgamated sandstone (St2).

The four facies present in the Stump Formation have repeated gradual transitions that reveal the arrangement of depositional environments on the siliciclastic wave-dominated shelf. Facies St1 (heterolithic shale) is the most basinward facies, and it is interpreted to have been deposited in the offshore transition zone. Facies St1 grades upwards into Facies St2 (amalgamated sandstone), interpreted to have been a lower

shoreface. Facies St2 grades upwards into Facies St3 (trough cross-stratified sandstone), interpreted to record deposition in the upper shoreface. Facies St3 grades upwards into Facies St4 (planar-laminated sandstone) and is interpreted to record deposition in the foreshore.

There are similarities between the facies model developed for the Stump Formation and the facies models for Jurassic strata in the Bighorn Basin, southwestern Wyoming, and northern Utah (Wilcox and Currie 2008; McMullen et al. 2014; Danise and Holland 2018). McMullen et al. (2014) has an equivalent to Facies St1, St2, and St3 (their Facies S2). McMullen et al. (2014) also report shell beds (their Facies S3). Danise and Holland (2018) both have equivalents to facies St1 (their Facies W3), St2 (W4), and St3 (W5). Both McMullen et al. (2014) and Danise and Holland (2018) report offshore environments and shell beds (their facies S1 and W1). Offshore environments are present within the Stump Formation and have been described in northern Utah (Facies Sr2 in Wilcox and Currie 2008), but are generally covered in the Wyoming Range. Wilcox and Currie also describe equivalent facies to St1 (their Sr3), St2 (Sr1), and St3 (Sr1).

The facies model developed here for the Stump Formation also bears strong resemblance to other siliciclastic wave-dominated shelf facies models (Clifton 2006), particularly the inner shelf (Facies St1, St2, St3, and St4). For example, on a Cretaceous wave-dominated shelf also deposited in a foreland basin of central Utah (Western Interior Seaway), offshore transition heterolithic sandstones pass upward through amalgamated sandstones deposited in the lower shoreface (Pattison 2018). This Cretaceous siliciclastic shelf continues landward through upper shoreface and foreshore environments. The difference between the Stump Formation and the Cretaceous shelf is the absence of

hummocky cross-stratification, indicating the Stump Formation was deposited in a lower-energy setting (Clifton 2006). The scarcity or absence of hummocky cross-stratification is observed across the Jurassic of Wyoming (Danise and Holland 2018).

SEQUENCE STRATIGRAPHY

In the Wyoming Range of southwestern Wyoming, the upper portion of the Giraffe Creek Member of Twin Creek Limestone, the Preuss Formation, and the Stump Formation form one partially complete depositional sequence bounded by a marine surface of forced regression at its base and capped by an unconformity below the Cretaceous Gannet Group (Fig. 13; Pipiringos and Imlay 1979). Because the outcrop exposure is relatively poor throughout the Wyoming Range, interpretation of the sequence-stratigraphic architecture below will focus on the nearly complete exposure at La Barge Creek, supplemented by well logs (Fig. 14).

Falling-Stage Systems Tract (FSST)

At La Barge Creek, the falling-stage systems tract is characterized by two closely spaced surfaces of forced regression, overlain by one abruptly shallowing-upward parasequence (~ 1 m into the Giraffe Creek Member at La Barge Creek, Fig. 13). Between the two surfaces of forced regression there is approximately 5 to 10 cm of lime mudstone interbedded with several very-thin, lenticular beds of ooid grainstone. These surfaces of forced regression are characterized by a sharp erosional base, overlain by a flat-pebble conglomerate also containing columnals of the crinoid *Isocrinus*, echinoid spines, mudstone intraclasts, and large-scale trough cross stratification (Figs. 7 and 13). This boundary lacks evidence for subaerial exposure (i.e. paleosol, paleokarst, patterned carbonate), and appears to be deposited in an entirely marine setting.

Overlying the upper surface of forced regression is a rapidly shallowing-upward parasequence that is characterized by a rapid transition from open shallow subtidal facies (Gc1) to ooid shoal facies (Gc2) with a sharp erosional base less than 1–1.5 m above the lowest surface of forced regression (located at approximately 2 m in the La Barge Creek column, Fig. 13). The surface of forced regression at the base of the ooid shoal facies has approximately 1–1.5 m of erosional relief (Fig. 13). The abrupt transition from open shallow subtidal faces (Gc1) to ooid shoal facies (Gc2) reflects decreasing accommodation throughout the falling-stage systems tract.

In well logs, the falling-stage systems tract is characterized by one or two abrupt shallowing-upward parasequences, each with a surface of forced regression at its base. This abrupt shallowing-upwards parasequence and surface of forced regression are recognized by a rapid transition from radioactive mudstone to less radioactive sands in less than 2 m (seen at the base of well logs 49-029-20535, 49-023-20158, 49-035-20659, and 49-023-20398, Fig. 15). This surface correlates updip in well 49-039-20018 to a sequence boundary and incised valley (Fig. 15). The incised valley fill is expressed by the abrupt transition from radioactive mudstones to less radioactive blocky sands. The strata above this surface display progradational to aggradational stacking, which suggests they overlie a surface of forced regression or sequence boundary, and that they are in the early lowstand systems tract. Surfaces of forced regression are not correlated along the two cross-sections because these surfaces may not be the same surfaces. Along depositional dip (from A–A′, Fig. 15), surfaces of forced regression would be expected to become progressively younger (Hunt and Tucker 1992).

Lowstand Systems Tract (LST)

Four parasequences displaying progradational to aggradational stacking record an increasing rate of accommodation in the early lowstand systems tract (Figs. 13–16). The first of these shallows upward from open shallow subtidal (Gc1) to mudflat (Gc2) facies, and the remaining three shallow upwards from peritidal to (Gc5) mudflat and mixed flat (Pr2) facies (located between 5 and 20 m in the La Barge Creek column, Fig. 13). At La Barge Creek, the middle to late lowstand systems tract consists of sandflat (Pr1) through mudflat (Pr3) facies forming four parasequences that are weakly developed and aggradationally stacked (located from approximately 20 to 100 m in the La Barge Creek column, Fig. 13). This interval is dominated by mixed flat facies (Pr2) with minor mudflat facies (Pr3; Fig. 13). In the middle to late lowstand, sandflat facies (Pr1) occur once (at approximately 70 m in the La Barge Creek column, Fig. 13), and it is less than 1.5 m thick. The late lowstand systems tract at La Barge Creek is characterized by four weakly retrogradationally stacked parasequences, reflecting an increasing rate of accommodation in the late lowstand. These parasequences shallow upwards from sand flat facies (Pr1) to mixed flat facies (Pr2; located from approximately 100–140 m in the La Barge Creek column, Fig. 13). The loss of shallow-water facies (mudflat) and the occurrence of deeper-water facies (sandflat) at the base of these parasequences indicate retrogradational stacking.

In well logs, the early lowstand systems tract consists of two to three parasequences with progradational to aggradational stacking (Figs. 15 and 16). The middle to late lowstand systems tract is represented by an aggradational sandy interval that generally has three to five poorly-developed shallowing-upwards parasequences

(Figs. 15 and 16). In this interval it is difficult to pick out individual parasequences along both cross-sections. Several marine shallowing-upward parasequences are well-developed in the depositionally downdip portions of the middle to late lowstand systems tract (well log 49-023-20398, Fig 14), and this well log is generally aggradationally stacked throughout this interval. Individual flooding surfaces cannot be correlated on either cross-section, probably owing to local variations in sedimentation and subsidence. Although individual flooding surfaces cannot be correlated, each well log shows well developed aggradational stacking, and the lowstand systems tract can be correlated along depositional dip and east to west (Figs. 15 and 16).

Transgressive Systems Tract (TST)

At La Barge Creek, the transgressive surface is a major marine flooding surface where mixed flat (Pr1) facies is overlain by a covered interval interpreted to be offshore or offshore transition (St1) facies (located at approximately 150 m in the La Barge Creek column, Fig. 13). The strata above this surface are interpreted to be retrogradationally stacked, which suggest they overlie the transgressive surface, and that they were deposited in the transgressive systems tract. Likewise, the maximum flooding surface is not visible in outcrop and its exact placement is unclear.

In well logs, the transgressive surface is the first large marine flooding surface overlying the aggradationally stacked sandy interval. It is clearly visible in every well log except well logs 49-023-20215 and 49-023-20590 (Fig. 16). Unlike parasequence-scale flooding surfaces, large marine flooding surfaces like the transgressive surface can be correlated along both cross-sections, and this transgressive surface is therefore used as the datum (Figs. 15 and 16). In well logs, the transgressive systems tract consists of two

to four retrogradationally stacked parasequences (Figs. 15 and 16). Although individual flooding surfaces cannot be confidentially correlated between well logs in the study area, retrogradational stacking is seen in every well log, and the transgressive systems tract can be traced with confidence throughout the study area (Figs. 15 and 16). The maximum flooding surface is recognized in well logs by the last flooding surface before parasequences become progradationally stacked. The maximum flooding surface is identifiable in every well log except two (well logs 49-023-2015 and 49-023-20591, Fig. 16), and it also can be correlated throughout the study area.

Highstand Systems Tract (HST)

At La Barge Creek, the highstand systems tract consists of offshore or offshore transition (St1) through foreshore (St4) facies that form four progradationally stacked parasequences (located from approximately 175–210 m in the La Barge Creek column, Fig. 13). The progradational stacking at La Barge Creek reflects the decreasing accommodation throughout the highstand systems tract. At La Barge Creek, the offshore unit (St1) in each parasequence of the highstand systems tract is covered.

In well logs, the highstand systems tract is generally represented by four to six progradationally stacked parasequences (Figs. 15 and 16). Similar to the other systems tracts, parasequence-scale flooding surfaces cannot be correlated confidentially along depositional dip or east to west (Figs. 15 and 16). Although individual flooding surfaces cannot be correlated, each well log shows progradational stacking, and the highstand systems tract can be correlated throughout the study area (Figs. 15 and 16).

Backstripping Results

Backstripping calculates a decompacted subsidence curve and provides an estimate of changes in accommodation though time (Sahagian and Holland 1991). There are several inherent sources of error, including estimates of time and water depth. For example, there is 1–1.5 m.y. of uncertainty associated with the timing of the stage boundaries for the Bajocian, Bathonian, Callovian, and Oxfordian (Cohen et al. 2018), all of which are used to estimate the timing of subsidence (Fig. 17). These uncertainties are reflected in the horizontal error bars in the subsidence curve. Additionally, estimates of water depth can have a large effect on the calculated subsidence curve. Overestimates of water depth will overestimate accommodation, whereas underestimating water depth will underestimate accommodation. The uncertainty in water depth is reflected by a red envelope that surrounds the subsidence curve, which shows the maximum and minimum accommodation, based on the maximum and minimum estimates of water depth implied by the facies (Fig. 17).

A decompacted subsidence curve from the Twin Creek Limestone, Preuss, and Stump formations provides an estimate of the subsidence history through the Middle to Late Jurassic at La Barge Creek (Fig. 17). This curve shows a sharp increase in accommodation rate in the middle to late Bathonian, followed by progressively slowing subsidence in the Callovian and Oxfordian. At La Barge Creek, accommodation rates shift from 0.025 m/k.y. during the Bajocian to mid Bathonian (170.3–167.2 Ma), to 0.1 m/k.y. in the late Bathonian. High accommodation rates in the middle to late Bathonian agree with the timing of peak subsidence rates in northern Utah (Bjerrum and Dorsey 1995). During the deposition of the Preuss Formation, accommodation rates decreased to

0.022 m/k.y. during the Callovian (165.7 to 163.5 Ma). During the deposition of the Stump Formation accommodation decreased even more to 0.01 m/k.y. from the late Callovian to early Oxfordian (163.5 Ma to 159 Ma).

Although the peak accommodation rate found at La Barge Creek is high, it likely underestimates the true peak rate of accommodation. The decompacted accommodation curve provides an estimate of the size and relative rate of subsidence through time, although there is uncertainty in the absolute rate because of the lack of absolute age data from the Twin Creek Limestone and Preuss and Stump formations. Backstripping likely calculates a minimum accommodation rate because a rate derived from backstripping averages the rate between data points. Most likely there would have been periods of rapid subsidence in the Middle to Late Jurassic followed by tectonic quiescence. This analysis would have averaged across those episodic periods of higher and lower accommodation rates.

DISCUSSION

Correlations and Sundance Chronostratigraphy

Although the sequence-stratigraphic architecture of the Middle and Upper Jurassic in the Bighorn Basin is well-characterized (Parcell and Williams 2005; McMullen et al. 2014; Clement and Holland 2016; Danise and Holland 2018), how these sequences correlate to the Stump and Preuss formations has not been previously determined. Existing biostratigraphic correlations and sequence-stratigraphic descriptions of the Middle to Upper Jurassic strata in the Bighorn Basin (Pipiringos and Imlay 1979; McMullen et al. 2014; Danise and Holland 2018), along with the sequence-stratigraphic

interpretation developed here, were used to correlate the Preuss and Stump formations to the Jurassic strata of the Bighorn Basin (Fig. 2).

Biostratigraphically, the Watton Canyon, Leeds Creek, and Giraffe Creek Members of the Twin Creek Formation correlate to the Canyon Spring, Stockade Beaver and Hullett Members of the Sundance Formation, based on the *Sigaloceras calloviense* and *Macrocephalites macrocephalus* ammonite zones (Fig. 2; Imlay 1980). Prior to the present study, the age of the Preuss Formation was poorly constrained because of a lack of fossils. The Preuss was thought to be Callovian and correlative to the Lak Member of the Sundance Formation because of its unconformable lower and upper contacts with the Giraffe Creek Member of the Twin Creek Limestone and the Stump Formation (Imlay 1952). The biostratigraphic correlations of Pipiringos and Imlay (1979) indicate that the Stump Formation is equivalent to the Redwater Shale Member of the Sundance Formation, based on the *Quenstedtoceras mariae* and *Cardioceras cordatum* ammonite zones (Fig. 2).

The sequence-stratigraphic architecture described here suggests that the Preuss Formation is conformable with both the underlying Giraffe Creek Member and the overlying Stump Formation. Biostratigraphically, the Giraffe Creek Member of the Twin Creek Limestone and the Stump Formation are equivalent to the Hulett and Redwater Members of the Sundance Formation (Pipiringos and Imlay 1979; Imlay 1980), which constrains the Preuss Formation as middle to upper Callovian and correlative to the J-4 sequence boundary (Kvale et al. 2001; Danise and Holland 2018). This suggests that during a period of subaerial exposure and the formation of the J-4 sequence boundary in

central Wyoming, the foredeep did not experience enough of a relative sea-level fall to record subaerial exposure.

Foreland Basin Sequence Stratigraphy

The sequence-stratigraphic architecture described in this study not only has important implications for the stratigraphic architecture of the Sundance Seaway, it has implications for understanding the stratigraphic architecture in other foreland basins. Posamentier and Allen (1993) predicted that the location of the shoreline in a foreland basin would have a strong control on the stratigraphic architecture. If the shoreline was in the high-accommodation zone (that is, the foredeep), no relative fall in sea level would occur during a eustatic fall because the rate of tectonic subsidence would be greater than the rate of eustatic sea level fall. Consequently, a correlative conformity would develop instead of an unconformity. If the shoreline was in the low-accommodation zone, such as the distal part of a foreland basin, and if subsidence was slower than the rate of eustatic sea-level fall, the shelf would be exposed, and a subaerial unconformity would form. It is important to note that the width of the high-accommodation zone will increase during times of thrusting and narrow during times of tectonic quiescence (Posamentier and Allen 1993; Decelles and Gilles 1996).

The predictions from this theoretical framework are reflected in the sequence-stratigraphic architecture of the Sundance Seaway from the early Callovian through Oxfordian. In the distal part of the foreland basin (the Bighorn Basin), this time period corresponds to a relative fall in sea level, subaerial exposure, and the formation of the J-4 unconformity (Danise and Holland 2018). This was followed by a period of relative sea-level rise and eventual progradation, forming the J-4 depositional sequence consisting of

the Redwater Shale and Windy Hill members of the Sundance Formation (McMullen et al. 2014; Danise and Holland 2018). During this period, in the high-accommodation zone of the foredeep in westernmost Wyoming and Idaho, the strata consists of a thick lowstand systems tract capped by a relatively thin transgressive and highstand systems tract (Fig. 13). This suggests that during the formation of the J-4 sequence boundary in central Wyoming, the lowstand systems tract was deposited in the rapidly subsiding foredeep, recorded by the Preuss Formation.

Significantly, the lowstand systems tract is bounded by a surface of forced regression at its base. The presence of a surface of forced regression and a lack of subaerial exposure is relevant because it suggests that the rate of subsidence was less than the rate of eustatic sea-level fall, causing a forced regression of shoreline, but that the rate of subsidence was high enough to prevent subaerial exposure. For a surface of forced regression to form, a portion of the foredeep must have been in the low-accommodation zone, suggesting that the width of the high-accommodation zone narrowed during quiescence. If the sequence was deposited in the distal portion of the basin (an even lower-accommodation zone), subaerial exposure and incision would have occurred, causing the formation of incised valleys and a sequence boundary (Posamentier and Allen 1993). This interpretation is supported on the east–west cross-section (well 49-039-20018, Fig. 16) and by the accommodation curve for La Barge Creek (Fig. 17). From east to west, the lowstand systems tract thickens by ~ 17 times from ~ 20 m at well log 49-023-20591 to over ~ 350 m at well log 49-023-20215 (Fig. 16). When the accommodation curve from La Barge Creek is compared with those calculated in the Bighorn and Wind River Basins (Danise and Holland 2018; Fig. 17), it suggests that the

total accommodation from the Middle to Late Bajocian through the Callovian was at least three times greater at La Barge Creek than the total accommodation at any location in the distal part of the basin (Danise and Holland 2018). It is possible that eustatic sea level may have been a primary control on the sequence stratigraphic architecture of the Sundance Seaway. Estimates of eustasy indicate there was a eustatic sea-level rise of 50 to 100 m during the Middle to Late Jurassic (Haq et al., 1987; Sahagian et al. 1996; Haq and Al-Qahtani 2005). If the maximum eustatic sea-level rise during the Middle to Late Jurassic is assumed, it would account for less than halve of the total accommodation at La Barge Creek, suggesting that tectonic subsidence was a higher order control on the sequence stratigraphic architecture of the Sundance Seaway (Fig. 17).

The sequence-stratigraphic architecture suggests that tectonic subsidence and the position of the shoreline within the high or low-accommodation zone played a primary control on the sequence-stratigraphic architecture in a foreland basin. During the Callovian, the Sundance Seaway experienced a relative fall in sea level (McMullen et al. 2014; Danise and Holland 2018). During this relative sea-level fall, the shoreline underwent forced regression, subaerially exposing the shelf and forming the J-4 unconformity (McMullen et al. 2014; Danise and Holland 2018). As the shoreline migrated downdip, it transitioned from the low-accommodation zone to a higher accommodation zone, where deposition was uninterrupted by an unconformity, and the lowstand systems tract was deposited during the initial rise in relative sea level. In the early Oxfordian, relative sea level continued to rise at an increasing rate, forming a transgressive systems tract in the foredeep and in the distal portions of the basin. In the early to middle Oxfordian, relative-sea rise continued, but at a decreasing rate, forming

the highstand systems tract throughout the basin. Additionally, Oxfordian rates of accommodation at La Barge Creek are similar to those in the distal portions of the basin (Danise and Holland 2018), when both gain ~ 20 m in accommodation. Although subsidence and the position of the shoreline are primary controls on the sequence-stratigraphic architecture of foreland basins, along-strike variations in sedimentation likely have a second-order or third-order control on stratigraphic architecture. This is reflected in the difficulty correlating higher-order (parasequence scale) flooding surfaces along strike or dip in the Wyoming Range.

CONCLUSIONS

1. The Giraffe Creek Member of the Twin Creek Limestone, the Preuss Formation, and the Stump Formation record three distinct facies associations that allow environmental reconstructions along depositional dip. The Giraffe Creek Member was deposited on a carbonate ramp, the Preuss Formation was deposited on a siliciclastic tidally-dominated coast, and the Stump Formation was deposited on a low-energy wave-dominated shelf.

2. In the Wyoming Range, the upper portion of the Giraffe Creek Member of the Twin Creek Limestone and the Preuss and Stump formations consitute one partially complete depositional sequence bounded by a surface of forced regression at its base and the sub-Cretaceous unconformity (K-1 of Pipiringos and O'Sullivan 1978) above. This depositional sequence is equivalent to the J-4 sequence in the Bighorn Basin as described by McMullen et al. (2014) and Danise and Holland (2018). The lowstand systems tract (Preuss Formation) is equivalent to the J-4 unconformity up-dip in the distal portion of

the basin, and the transgressive and highstand systems tracts (Stump Formation) are equivalent to the Redwater and Windy Hill Members of the Sundance Formation.

3. The results of this study support the theoretical framework for the sequence-stratigraphic architecture of foreland basins proposed by Posamentier and Allen (1993). As they suggest, tectonic subsidence and the position of the shoreline in the high or low-accommodation zone are the primary controls on the sequence-stratigraphic architecture of foreland basins.

CHAPTER 3

CONCLUSIONS

The Giraffe Creek Member of the Twin Creek Limestone, the Preuss Formation, and the Stump Formation record three distinct facies associations with characteristic sets of lithologies, bedding, sedimentary structures, fossils, and facies contacts that allow environmental reconstructions along depositional dip. The Giraffe Creek Member was deposited on a carbonate ramp with shallowing upward associations consisting of open shallow subtidal facies (Gc1,) ooid shoal facies (Gc2), restricted shallow subtidal facies (Gc3 and Gc4), intertidal flat facies (Gc5), and desert flat facies (Gc6). The Preuss Formation was deposited on a siliciclastic, tidally-dominated coast and includes sand flat facies (Pr1), mixed flat facies (Pr2), and mud flat facies (Pr3). The Stump Formation was deposited on a low-energy, wave-dominated shelf and contains offshore to offshore transition facies (St1), lower shoreface facies (St2), upper shoreface facies (St3), and foreshore facies (St4).

In the Wyoming Range of Wyoming and Idaho, the upper portion of the Giraffe Creek Member, the Preuss Formation, and the Stump Formation constitute one partially complete depositional sequence. This depositional sequence is bounded by a surface of forced regression at its base and an unconformity at its top, overlain by the Cretaceous Gannet Group (Pipiringos and Imlay 1979). This depositional sequence correlates to the J-4 sequence in the Bighorn Basin as described by McMullen et al. (2014) and Danise and Holland (2018). The lowstand systems tract of this sequence is represented by the Preuss Formation, and it is equivalent to the J-4 unconformity up-dip in the distal portion

of the Sundance Seaway. The transgressive and highstand systems tracts are represented by the Stump Formation, and they are equivalent to the Redwater and Windy Hill members of the Sundance Formation.

The sequence-stratigraphic architecture of the Sundance Seaway suggests that tectonic subsidence and the position of the shoreline in the high or low-accommodation zone are the primary controls on the sequence-stratigraphic architecture of a foreland basin, which supports the theoretical framework proposed by Posamentier and Allen (1993). During a fall in relative sea level and the formation of the J-4 unconformity up dip (within the low-accommodation zone), the shoreline migrated down dip and deposited the lowstand systems tract (Preuss Formation) in the foredeep (a higher-accommodation zone), where deposition was uninterrupted by a subaerial unconformity. Following the initial rise in relative sea level and the deposition of the lowstand systems tract, relative sea level continued to rise and form the transgressive and highstand systems tracts throughout the Sundance Seaway.

REFERENCES

AGHAEI, A., MAHBOUBI, A., MOUSSAVI-HARAMI, R., HEUBECK, C., AND NADJAFI, M., 2013, Facies analysis and sequence stratigraphy of an Upper Jurassic carbonate ramp in the Eastern Alborz range and Binalud Mountains, NE Iran: Facies, v. 59, p. 863–889.

AITKEN, J.F., AND FLINT, S.S., 1995, The application of high-resolution sequence stratigraphy to fluvial systems: a case study from the Upper Carboniferous Breathitt Group, eastern Kentucky, USA: Sedimentology, v. 42, p. 3–30.

ALEXANDER, C.R., DEMASTER, D.J., PARK, Y., AND PARK, S., 1991, Macrotidal mudflats of the southwestern Korean coast: a model for interpretation of intertidal deposits: Journal of Sedimentary Petrology, v. 61, p. 805–824.

BACHMANN, M., AND HIRSCH, F., 2006, Lower Cretaceous carbonate platform of the eastern Levant (Galilee and the Golan Heights): stratigraphy and second-order sea-level change: Cretaceous Research, v. 27, p. 487–512.

BEAUMONT, C., QUINLAN, G., AND HAMILTON, J., 1988, Orogeny and stratigraphy: numerical models of the Paleozoic in eastern interior of North America: Tectonics, v. 7, p. 389–416.

BILBEY, S.A., HALL E., AND WELLES S.P., 1990, Pliosaurian plesiosaur found in Redwater Member of the Stump Formation (Jurassic-Oxfordian) of northeastern Utah: Journal of Vertebrate Paleontology, v. 10, p. 14A.

BILBEY, S.A., MICKELSON, D.L., HALL, J.E., KIRKLAND, J.I., MADSEN, S.K., BLACKSHEAR, B., AND TODD, C., 2005, Vertebrate ichnofossils from the Upper Jurassic Stump to Morrison transition; Flaming Gorge Reservoir, Utah: Utah Geological Association Publication 33, p. 111–123.

BJERRUM, C.J., AND DORSEY, R.J., 1995, Tectonic controls on deposition of Middle Jurassic strata in a retroarc foreland basin, Utah-Idaho trough, western interior, United States: Tectonics, v. 14, p. 962–978.

BLAKEY, R.C., 2015, Western Interior Seaway: Jurassic and Cretaceous epicontinental seas of North America. http://cpgeosystems.com/wispaleogeography.html. Accessed 6 January 2015.

BREWER, R., 1960, Cutans: their definition, recognition, and interpretation: European Journal of Soil Science, v. 11, p. 280–292.

BURCHETTE, T.P., AND WRIGHT, V.P., 1992, Carbonate ramp depositional systems: Sedimentary Geology, v. 79, p. 3–57.

BURCHETTE, T.P., WRIGHT, V.P., AND FAULKNER, T.J., 1990, Oolitic sandbody depositional models and geometries, Mississippian of southwest Britain: implications for petroleum exploration in carbonate ramp settings: Sedimentary Geology, v. 68, p. 87–115.

CHURE, D.J., 1993, The first record of ichthyosaurs in Utah: Brigham Young Geology Studies, v. 39, p. 65–69.

CLEMENT, A.M., AND HOLLAND, S.M., 2016, Sequence stratigraphic context of extensive basin-margin evaporites: Middle Jurassic Gypsum Spring Formation, Wyoming, USA: Journal of Sedimentary Research, v. 86, p. 965–981.

CLIFTON, H.E., 2006, A reexamination of facies models for clastic shorelines: Society of Economic Paleontologists and Mineralogists Special Publication 84, p. 293–337.

COHEN, K.M., HARPER, D.A.T., AND GIBBARD, P.L., 2018, ICS International Chronostratigraphic Chart 2018/08: International Commission on Stratigraphy, IUGS. www.stratigraphy.org. Accessed 27 March 2019.

COOK, P.S., 2016, Sedimentology and stratigraphy of the Middle Jurassic Preuss Sandstone in northern Utah and eastern Idaho [M.S. Thesis]: Brigham Young University.

DALRYMPLE, R.W., 2010, Tidal depositional systems, *in* James, N.P., and Dalrymple, R.W., eds., Facies Models 4: Dalhousie, Geological Association of Canada, p. 201–231.

DANISE, S., AND HOLLAND, S.M., 2017, Faunal response to sea level and climate change in a short-lived seaway: Jurassic of the Western Interior, USA: Palaeontology, v. 60, p. 213–232.

DANISE, S., AND HOLLAND, S.M., 2018, A sequence stratigraphic framework for the Middle to Late Jurassic of the Sundance Seaway, Wyoming: implications for correlation, basin evolution, and climate change: The Journal of Geology, v. 126, p. 371–405.

DECELLES, P.G., AND GILES, K.A., 1996, Foreland basin systems: Basin Research, v. 8, p. 105–123.

DESJARDINS, P.R., BUATOIS, L.A., AND MÁNGANO, M. G., 2012a, Tidal flats and subtidal sand bodies, *in* Knaust, D., and Bromley, R.G., eds., Trace Fossils as Indicators of Sedimentary Environments: Developments in Sedimentology, v. 64, p. 529–561.

DESJARDINS, P.R., BUATOIS, L.A., PRATT, B.R., AND MÁNGANO, M.G., 2012b, Forced regressive tidal flats: response to sea level in tide-dominated settings: Journal of Sedimentary Research, v. 82, p. 149–162.

DROSER, M.L., AND BOTTJER, D.J., 1993, Trends and patterns of Phanerozoic ichnofabrics: Annual Review of Earth and Planetary Sciences, v. 21, p. 205–225.

EKDALE, A.A., 1988, Pitfalls of paleobathymetric interpretations based on trace fossil assemblages: Palaios, v. 3, p. 464–472.

ELRICK, M., AND READ, J.F., 1991, Cyclic ramp-to-basin carbonate deposits, Lower Mississippian, Wyoming and Montana: a combined field and computer modeling study: Journal of Sedimentary Petrology, v. 61, p. 1194–1224.

EVANS, G., SCHMIDT, V., BUSH, P., AND NELSON, H., 1969, Stratigraphy and geologic history of the sabkha, Abu Dhabi, Persian Gulf: Sedimentology, v. 12, p. 145–159.

FELDMANN, R.M., AND TITUS, A.L., 2006, *Eryma jungostrix* n. sp. (Decapoda; Erymidae) from the Redwater Shale Member of the Stump Formation (Jurassic; Oxfordian) of Utah: Journal of Crustacean Biology, v. 26, p. 63–68.

FLEMMING, B.W., 2012, Siliciclastic back-barrier tidal flats, *in* Davis, R.A., and Dalrymple R.W., eds., Principles of Tidal Sedimentology: Dordrecht, Springer, p. 231–267.

FLÜGEL, E., 2010, Microfacies of Carbonate Rocks: Analysis, Interpretation and Application, Second Edition: Berlin, Springer-Verlag, 984 p.

FREBOLD, H., MOUNTJOY, E., AND REED, R., 1958, The Oxfordian beds of the Jurassic Fernie Group, Alberta and British Columbia: Geological Survey of Canada Bulletin 53.

GORNITZ, V.M., AND SCHREIBER, B.C., 1981, Displacive halite hoppers from the Dead Sea: some implications for ancient evaporite deposits: Journal of Sedimentary Petrology, v. 51, p. 787–794.

HAQ, B.U., HARDENBOL, J., AND VAIL, P.R., 1987, Chronology of fluctuating sea levels since the Triassic: Science, v. 235, p. 1156–1167.

HAQ, B.U., AND AL-QAHTANI, A.M., 2005, Phanerozoic cycles of sea-level chance on the Arabian Platform: GeoArabia, v. 10, p. 127–160.

HILEMAN, M.E., 1973, Stratigraphy and paleoenvironmental analysis of the Upper Jurassic Preuss and Stump formations, western Wyoming and southeastern Idaho [Ph.D. thesis]: Ann Arbor, University of Michigan.

HOWARD, J.D., AND REINECK, H.E., 1981, Depositional facies of high-energy beach-to-offshore sequence: comparison with low-energy sequence: American Association of Petroleum Geologists Bulletin, v. 65, p. 807–830.

HOWES, B.J., 2017, Sequence stratigraphic expression of flexural subsidence: Middle Jurassic Twin Creek Limestone [M.S. thesis]: Athens, University of Georgia.

HUGHES, Z.J., 2012, Tidal channels on tidal flats and marshes, *in* Davis Jr., R.A., and Dalrymple, R.W., eds., Principles of Tidal Sedimentology: Dordrecht, Springer, p. 269–300.

HUNT, D., AND TUCKER, M.E., 1992, Stranded parasequences and the forced regressive wedge systems tract: deposition during bas-level fall: Sedimentary Geology, v. 81, p. 1–9.

HUNT MOUNTAIN SOFTWARE, 2017, Backstrip 1.0. http://www.huntmountainsoftware.com/html/backstrip.html. Accessed 4 January 2019.

IMLAY, R.W., 1952, Marine origin of Preuss Sandstone of Idaho, Wyoming, and Utah: American Association of Petroleum Geologists Bulletin, v. 36, p. 1735–1753.

IMLAY, R.W., 1980, Jurassic paleobiogeography of the conterminous United States in its continental setting: U.S. Geological Survey Professional Paper 1062.

IMLAY, R.W., 1982, Jurassic (Oxfordian and late Callovian) ammonites from the western interior region of the United States: U.S. Geological Survey Professional Paper 1232.

KENDALL, A.C., 2010, Marine evaporites, *in* James, N.P., and Dalrymple, R.W., eds., Facies Models 4: St. John's, Geological Association of Canada, p. 541–576.

KOCUREK, G., AND DOTT, R.H., 1983, Jurassic paleogeography and paleoclimate of the central and southern Rocky Mountains region, *in* Reynolds, M.W., and Dolly, E.D., eds., Mesozoic Paleogeography of the West-Central United States: Society of Economic Paleontologists and Mineralogists, Rocky Mountain Section, p. 101–16.

KVALE, E.P., JOHNSON, A.D., MICKELSON, D.L., KELLER, K., FURER, L.C., AND ARCHER, A.W., 2001, Middle Jurassic (Bajocian and Bathonian) dinosaur megatracksites, Bighorn Basin, Wyoming, USA: Palaios, v. 16, p. 233–254.

MACK, G.H., AND JAMES, W.C., 1994, Paleoclimate and the global distribution of paleosols: The Journal of Geology, v. 102, p. 360–366.

MAYNARD, J.B., 1982, Extension of Berner's "New geochemical classification of sedimentary environments" to ancient sediments: Journal of Sedimentary Research, v. 54, p. 1325–1331.

MCILROY, D., FLINT, S., HOWELL, J.A., AND TIMMS, N., 2005, Sedimentology of the tide-dominated Jurassic Lajas Formation, Neuquén Basin, Argentina, *in* Veiga, G.D., Spalletti, L.A., Howell, J.A., and Schwarz, E., eds., The Neuquén Basin, Argentina: A Case Study in Sequence Stratigraphy and Basin Dynamics: Geological Society, London Special Publications 252, p. 83–107.

MCMULLEN, S.K., HOLLAND, S.M., AND O'KEEFE, F.R., 2014, The occurrence of vertebrate and invertebrate fossils in a sequence stratigraphic context: the Jurassic Sundance Formation, Bighorn Basin, Wyoming, USA: Palaios, v. 29, p. 277–294.

MELLERE, D., 1994, Sequential development of an estuarine valley fill: the Twowells Tongue of the Dakota Sandstone, Acoma Basin, New Mexico: Journal of Sedimentary Research, v. B64, p. 500–515.

MIALL, A.D., 1977, Lithofacies types and vertical profile models in braided river deposits: a summary, *in* Miall, A.D. ed., Fluvial Sedimentology: Canadian Society of Petroleum Geologists Memoir 5, p. 597–604.

MIALL, A.D., 1985, Architectural-element analysis: a new method of facies analysis applied to fluvial deposits: Earth-Science Reviews, v. 22, p. 261–308.

MIALL, A.D., 2014, Fluvial Depositional Systems: Berlin, Springer, 316 p.

NOFFKE, N., ERIKSSON, K.A., HAZEN, R.M., AND SIMPSON, E.L., 2006, A new window into Early Archean life: microbial mats in Earth's oldest siliciclastic tidal deposits (3.2 Ga Moodies Group, South Africa): Geology, v. 34, p. 253–356.

PARCELL, W. C., AND WILLIAMS, M. K., 2005, Mixed sediment deposition in a retro-arc foreland basin: lower Ellis Group (Middle Jurassic), Wyoming and Montana, USA: Sedimentary Geology, v. 177, p. 175–194.

PATTISON, S.A.J., 2018, Rethinking the incised-valley fill paradigm for Campanian Book Cliffs strata, Utah-Colorado, U.S.A.: evidence for discrete parasequence-scale, shoreface-incised channel fills: Journal of Sedimentary Research, v. 88, p. 1381–1412.

PEMBERTON, S.G., VAN WAGONER, J.C., AND WACH, G.D., 1992, Ichnofacies of a wave-dominated shoreline, *in* Pemberton, S.G., ed., Applications of Ichnology to Petroleum Exploration—A Core Workshop: SEPM Core Workshop 17, p. 339–382.

PIPIRINGOS, G.N., AND IMLAY, R.W., 1979, Lithology and subdivisions of the Jurassic Stump Formation in southeastern Idaho and adjoining areas: U.S. Geological Survey Professional Paper 1035-C.

PIPIRINGOS, G.N., AND O'SULLIVAN, R.B., 1978, Principal unconformities in Triassic and Jurassic rocks, western interior United States: a preliminary survey: U.S. Geological Survey Professional Paper 1035-A.

PLUMMER, P., AND GOSTIN, V., 1981, Shrinkage cracks: desiccation or synaeresis?: Journal of Sedimentary Petrology, v. 51, p. 1147–1156.

POPE, M.C., HOLLAND, S.M., AND PATZKOWSKY M.E., 2009, The Cincinnati Arch: a stationary peripheral bulge during the Late Ordovician, *in* Swart, S.K., Eberli, G.P., McKenzie, J.A., eds., Perspectives in Carbonate Geology: A Tribute to the Career of Robert Nathan Ginsburg: IAS Special Publication 41, p. 255–275.

POSAMENTIER, H.W., AND ALLEN, G.P., 1993, Siliclastic sequence stratigraphic patterns in foreland ramp-type basins: Geology, v. 21, p. 455–459.

SAHAGIAN, D.L., AND HOLLAND, S.M., 1991, Eustatic sea-level curve based on a stable frame of reference: preliminary results: Geology, v. 19, p. 1209–1212.

SAHAGIAN, D.L., PINOUS, O., OLFERIEV, A., AND ZAKHAROV, V., 1996, Eustatic curve for the Middle Jurassic—Cretaceous based on Russian Platform and Siberian stratigraphy: zonal resolution: American Association of Petroleum Geologists Bulletin, v. 80, p. 1433–1458.

SCHUCHERT, C., 1923, Sites and nature of the North American geosynclines: Geological Society of America Bulletin, v. 34, p. 151–230.

SIMONE, L., 1980, Ooids: a review: Earth-Science Reviews, v. 16, p. 319–355.

SMITH, L.B. AND READ, J.F., 2001, Discrimination of the effects of eustasy, tectonics and climate on Upper Mississippian mixed carbonates and siliciclastic sequences, Illinois Basin, USA: Journal of Sedimentary Research, v. 71, p. 985–1002.

VAIL, P.R., HARDENBOL, J., AND TODD, R.G., 1984, Jurassic unconformities, chronostratigraphy, and sea-level changes from seismic stratigraphy and biostratigraphy, *in* Schlee, J.S., ed., Interregional Unconformities and Hydrocarbon Accumulation: American Association of Petroleum Geologists Memoir 36, p. 129–144.

VAIL, P.R., MITCHUM, R.M., JR., AND THOMPSON, S., III, 1977, Seismic stratigraphy and global changes of sea level, part 3: relative changes of sea level from costal onlap, *in* Payton, C.E., ed., Seismic Stratigraphy—Applications to Hydrocarbon Exploration: American Association of Petroleum Geologists Memoir 26 p. 63–81.

VAN WAGONER, J.C., 1995, Sequence stratigraphy and marine to nonmarine facies architecture of foreland basin strata, Book Cliffs, Utah, U.S.A., *in* Van Wagoner, J.C., and Bertram, G.T., eds., Sequence Stratigraphy of Foreland Basin Deposits,

Outcrop and Subsurface Examples from the Cretaceous of North America: American Association of Petroleum Geologists Memoir 64, p. 137–223.

VAN WAGONER, J.C., AND BERTRAM, G.T., 1995, Sequence Stratigraphy of Foreland Basin Deposits, Outcrop and Subsurface Examples from the Cretaceous of North America: American Association of Petroleum Geologists Memoir 64.

VAN WAGONER, J.C., MITCHUM, R.M., CAMPION, K.M., AND RAHMANIAN, V.D., 1990, Siliciclastic Sequence Stratigraphy in Well Logs, Cores, and Outcrops: Concepts for High-Resolution Correlation of Time and Facies: American Association of Petroleum Geologists Methods in Exploration Series 7, 55 p.

WARREN, J.K., AND KENDALL, C.G.ST.C., 1985, Comparison of sequences formed in marine sabkha (subaerial) and salina (subaqueous) settings: modern and ancient: American Association of Petroleum Geologists Bulletin, v. 69, p. 1013–1023.

WATTS, A.B., 1988, Gravity anomalies, crustal structure and flexure of the lithosphere at the Baltimore Canyon Trough: Earth and Planetary Science Letters, v. 89, p. 221–238.

WILCOX, W.T., AND CURRIE, B.S., 2008, Sequence stratigraphy of the Jurassic Curtis, Summerville, and Stump formations, eastern Utah and northwest Colorado: Utah Geological Association Publication 37, p. 9–42.

WYOMING OIL AND GAS CONSERVATION COMMISSION, 2018, WOGCC data. http://pipeline.wyo.gov/legacywogcce.cfm. Accessed 10 October 2018.

TABLES

Table 1. Facies Associations of the Giraffe Creek Member of the Twin Creek Limestone

Facies association and interpretation	Lithology and bedding	Sedimentary structures	Fossils	Context
Gc1, Heterolithic Skeletal Ooid Grainstone	**Skeletal ooidal grainstone in very thin beds, planar-laminated lime mudstone in very thin beds**, grainstone beds are lenticular but are increasingly amalgamated upwards; **coarsens upwards**	Lime mudstone is generally planar laminated; grainstone contain abundant vortex ripples and small-scale trough cross stratification locally large-scale trough cross stratification	Abundant crinoid stems (*Isocrinus*), locally echinoid spines and plates	Facies is found on all but westernmost thrust sheets in the study area. Facies grades upwards into Facies GC2.
Gc2, Ooid Grainstone	Skeletal **ooidal grainstone** in very thin to medium beds; lime mudstone intraclasts and shell lags often occur at set boundaries	**Abundant large-scale trough cross** stratification, with intraclasts at set boundaries	Locally crinoid stems (*Isocrinus*)	Facies is found on all but westernmost thrust sheets in the study area. Facies gradationally overlies Facies Gc1, grades upwards into Facies Gc3.
Gc3, Heterolithic Carbonate Mudstone	**Planar-laminated lime mudstone in very thin beds skeletal ooidal grainstone in very thin beds.** Grainstone beds are lenticular but are decreasingly amalgamated upwards. **Facies fines upwards**	Lime mudstone is generally planar laminated; grainstone contain abundant vortex ripples. Small-scale trough cross stratification and megaripples locally present	Abundant crinoid stems (*Isocrinus*)	Facies is found on all thrust sheets in the study area. Facies gradationally overlies facies Gc2, grades upwards into facies Gc4.

GC4, Planar-laminated Lime Mudstone	Planar-laminated dolomitic **lime mudstone in very thin beds**	**Planar-laminated**, locally stromatolitic to algal lamination	Unfossiliferous	Facies is found on all but westernmost thrust sheets in the study area. **Facies** gradationally **overlies Facies Gc3**, grades upwards into Facies Gc5.
Gc5, Dolomitic Lime Mudstone	Planar-laminated dolomitic lime mudstone	Planar-laminated, commonly contains stromatolitic to algal lamination, **desiccation cracks**, current and wave ripple lamination, dewatering structures, and rain-drop impressions	Unfossiliferous	Facies is found on all but westernmost thrust sheets in the study area. Facies gradationally overlies Facies Gc4, grades upwards into Facies Gc6.
Gc6, Red Siltstone	**Sandy siltstone in very thin beds**, bioturbated	**Bioturbated**, small (<1 cm) anhydrite pseudomorphs	Unfossiliferous	Facies is found on all but westernmost thrust sheets in the study area. Facies gradationally overlies Facies Gc5.

Gc7, Gypsum-rich Red Siltstone	Sandy siltstone in very thin beds	Wavy lamination, **anhydrite crystals in very thin beds**, anhydrite crystal mush, **chicken-wire texture**	Unfossiliferous	Facies is not found at any locality but the Cabin Creek locality. Facies gradationally overlies Facies Gc5.

Table 2. Facies Associations of the Preuss Formation and the Curtis Member of the Stump Formation

Facies association and interpretation	Lithology and bedding	Sedimentary structures	Context
Pr1, Cross-bedded Sandstone	Very fine-grained to fine-grained sandstone in thin to medium beds, mudstone rip-up clasts are common; **facies fine upwards with increasing mud and bioturbation**	**Abundant ripple lamination,** both current and wave-generated forms; **climbing ripples**, 2-D current ripples, 3-D current ripples, vortex ripples, and **large-scale trough cross** stratification common	Facies is found throughout the study area. Facies grades upwards into Facies Pr2.
Pr2, Heterolithic Silty Sandstone	Silty very fine-grained sandstone in very thin beds, interbedded with mudstone in very thin beds. **Facies fines upwards with increasing mud.** Facies can be massively bedded and so heavily bioturbated (ii4–5) that no bedding planes are visible	**Wavy and flaser bedding,** extensive ripple lamination, both wave and current generated forms, **desiccation cracks, halite casts**, mudstone intraclasts, 2-D current ripples, 3-D current ripples, vortex ripples, and anhydrite or pseudomorph nodules are common, locally contains *Skolithos*	Facies is found throughout the study area. Facies gradationally overlies Facies Pr1, grades upwards into Facies Pr3. On the eastern thrust sheets, facies is heavily bioturbated where it gradationally overlies Facies Pr1 and becomes more heterolithic until it grades upwards into facies Pr3. On the western thrust sheets, facies is heterolithic where it gradationally overlies Facies Pr1.

Pr3, Red Mudstone	**Mudstone in very thin beds**, interbedded with silty very fine-grained sandstone in very thin beds	Planar-laminated; locally with halite casts and desiccation cracks. Sandstone beds are generally planar laminated, some are locally ripple-laminated	Facies is found throughout the study area. Facies gradationally overlies Facies Pr2.
Pr4, Red Silty Sandstone	Silty very fine-grained sandstone in very thin beds, heavily bioturbated, no bedding visible; gypsic nodular paleosol	**Abundant cutans and small (>1 cm) anhydrite nodules**; large anhydrite nodules are found locally	Facies found only of the westernmost thrust sheets in the study area; gradationally overlies Facies Pr5.
Pr5, Erosional-Based Sandstone	Fine to medium-grained sandstone in thin to medium beds, facies always has an **erosional base and fines upwards with increasing proportions of silt;** locally contains conglomeratic channel lag with an average clast size of 1.5–2 cm and a maximum size of 4 cm	**Commonly tabular-cross stratified, trough cross stratified**, and contains planar lamination and current ripples	Facies found only on the westernmost thrust sheets in the study area; grades upwards into Facies Pr4.

Table 3. Facies Associations of the Redwater Member of the Stump Formation

Facies association and interpretation	Lithology and bedding	Sedimentary structures	Context
St1, Heterolithic Shale	**Heterolithic**, very thinly planar-laminated shale interbedded with very thin to thin beds of very fine to fine-grained sandstone; sandstone beds are **lenticular or isolated but increase in number and amalgamation** upwards**, coarsens upwards**	Abundant **2-D current and vortex ripples**, wave-ripple and current-ripple cross stratification	Facies is found throughout the study area. Facies grades upwards into Facies St2. Facies is covered at La Barge Creek.
St2, Amalgamated Sandstone	Very fine to fine-grained sandstone in thin to medium **tabular beds**; heavily bioturbated	Abundant ***Ophiomorpha***	Facies is found throughout the study area. Facies gradationally overlies Facies St1; grades upwards into Facies St3.
St3, Trough Cross-Stratified Sandstone	Very fine to fine-grained sandstone in thin to medium beds; beds thin upwards	**Abundant large-scale trough cross stratification**, some *Ophiomorpha* present, but generally void of bioturbation	Facies is found throughout the study area. Facies gradationally overlies Facies St2 and grades upwards into Facies St4.

St4, Planar-Laminated Sandstone	Very fine to fine-grained sandstone in thin to **very thin beds**	**Abundant planar lamination**, possibly seaward inclined laminae, vortex ripples and parting lineation found locally	Facies observed only at La Barge Creek. Facies gradationally overlies Facies St3.

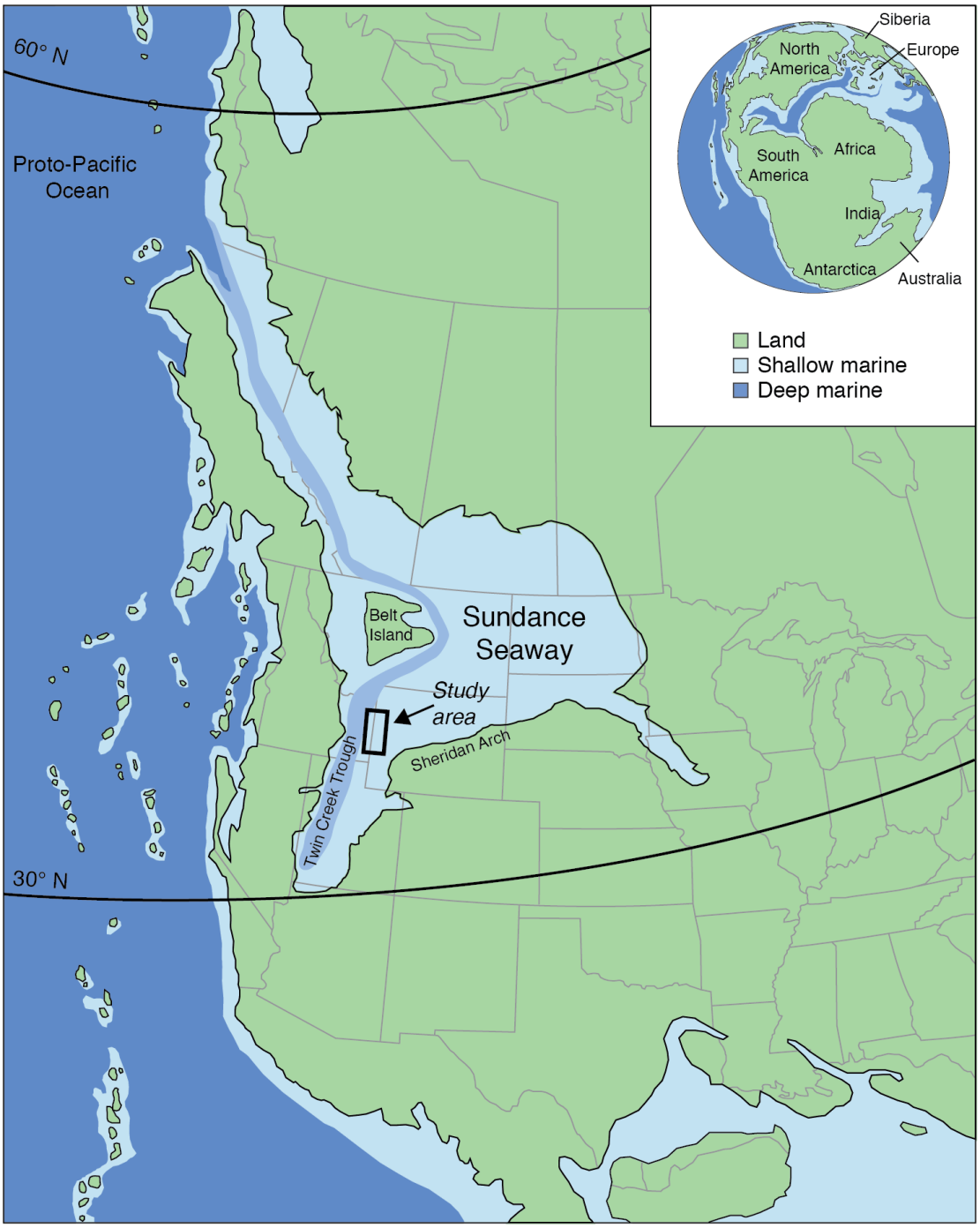
60° N
Proto-Pacific Ocean
Belt Island
Sundance Seaway
Study area
Sheridan Arch
Twin Creek Trough
30° N
Siberia
North America
Europe
Africa
South America
India
Antarctica
Australia
Land
Shallow marine
Deep marine

Fig.1— Paleogeographic reconstruction of western North America during the Bajocian Stage (~170 Ma), modified from Clement and Holland (2016) and based on the paleogeographic reconstruction of Blakey (2015). Box in western Wyoming indicates location of study area shown in Fig. 5.

western Wyoming
central Wyoming
Upper Jurassic
Middle Jurassic
Kim.
Oxfordian
Callovian
Bathonian
Bajocian
157.3 Ma
163.5
166.1
168.3
170.3
Biostratigraphic Zone
Cardioceras cordatum
Quenstedto. mariae
Quenstedto. lamberti
Pelto. athleta
Kosmo. jason
Sigaloceras calloviense
Macrocephalites macrocephalus
Clydoni. discus
Oppelia aspidoides
Tulites subcontractus
Zigzagiceras zigzag
Gracilis. progracilis
Parkins. parkinsoni
Garant. garantiana
Streno. subfurcatum
Stephano. humphriesianum
Stump Formation
Redwater Shale Member
Curtis
Curtis
Preuss Fm.
Twin Creek Limestone
Giraffe Creek Member
Leeds Creek Member
Watton Canyon Member
Boundary Ridge Member
Rich Member
Sliderock Member
Gypsum Spring Member
unconformities and sequences
Morrison Formation
Windy Hill Sandstone
Redwater Shale
Pine Butte
upper Hulett
lower & middle Hulett
Lak
Stockade Beaver Shale
Hulett
Canyon Springs
Canyon Springs Ss.
upper
middle
lower
Sundance Formation
upper
lower
Gypsum Spring Formation
J-4
J-3
J-2a
J-2
J-1b
J-1a
J-1
carbonate ramp
gypsum
siliciclastic wave-dominated shelf
siliciclastic desert
siliciclastic tidal coast
siliciclastic terrestrial

Fig.2.— Chronostratigraphic chart for the Middle and Upper Jurassic of western and central Wyoming, modified from Howes (2017) and Danise and Holland (2018). Biostratigraphy based on Imlay (1982). Ages based on Cohen et al. (2018).

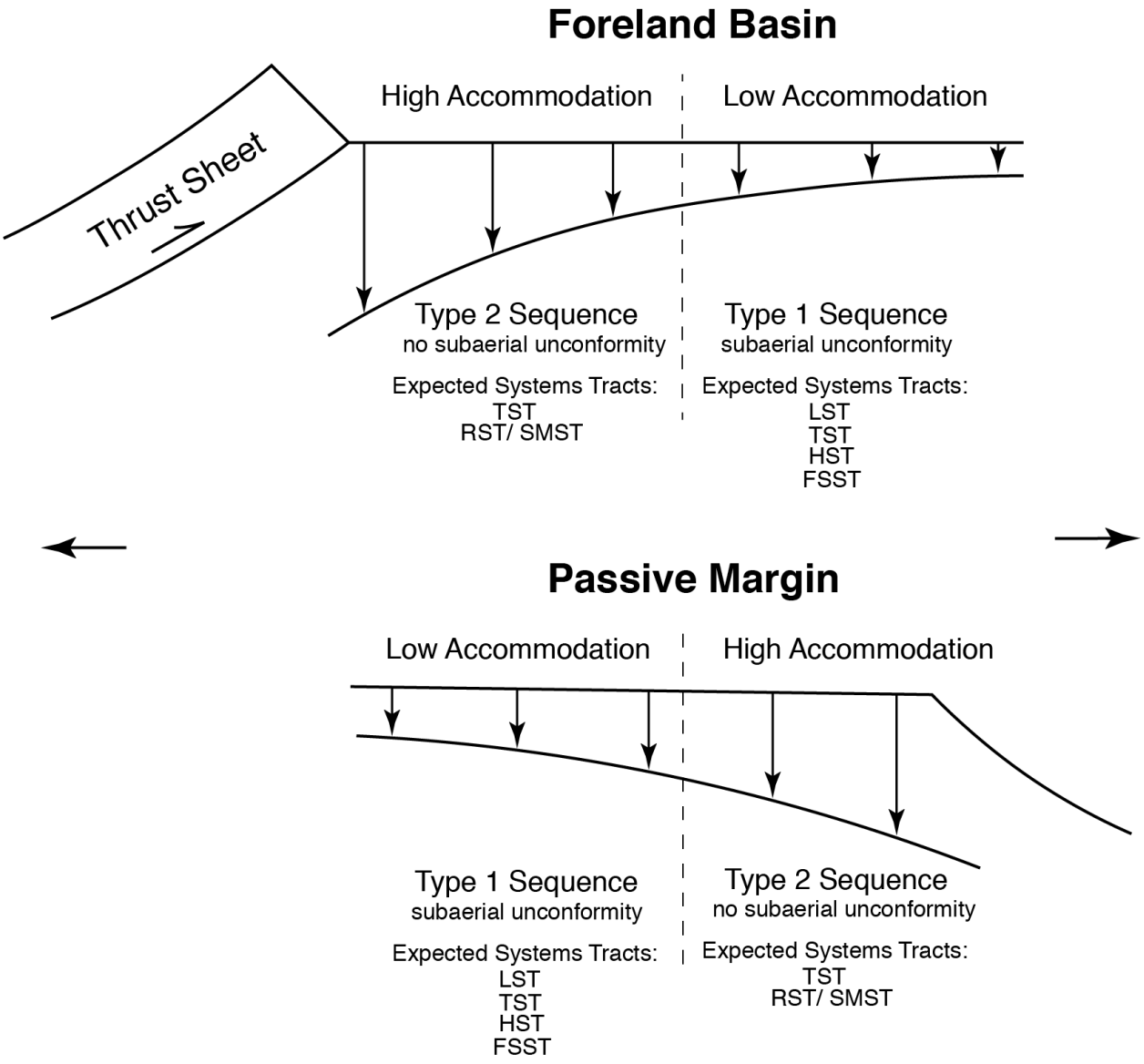
Foreland Basin
High Accommodation
Low Accommodation
Thrust Sheet
Type 2 Sequence
no subaerial unconformity
Expected Systems Tracts:
TST
RST/ SMST
Type 1 Sequence
subaerial unconformity
Expected Systems Tracts:
LST
TST
HST
FSST
Passive Margin
Low Accommodation
High Accommodation
Type 1 Sequence
subaerial unconformity
Expected Systems Tracts:
LST
TST
HST
FSST
Type 2 Sequence
no subaerial unconformity
Expected Systems Tracts:
TST
RST/ SMST

Fig.3.— Schematic sections across a foreland basin and a passive continental margin illustrating the contrasting subsidence patterns. Modified from Posamentier and Allen (1993).

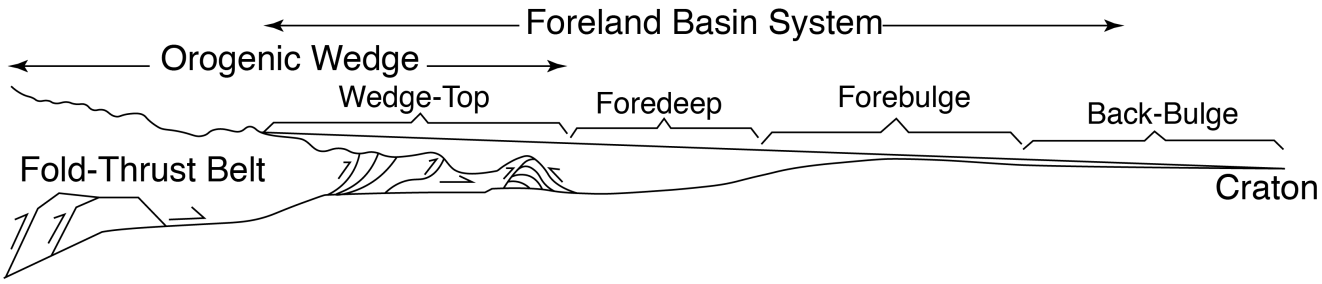
Foreland Basin System
Orogenic Wedge
Wedge-Top
Foredeep
Forebulge
Back-Bulge
Fold-Thrust Belt
Craton

Fig.4.— Schematic cross-section of a foreland basin system. Modified from DeCelles and Giles (1996). The amount of subsidence in the back-bulge is so small that it cannot be show at this scale (Pope et al. 2009).

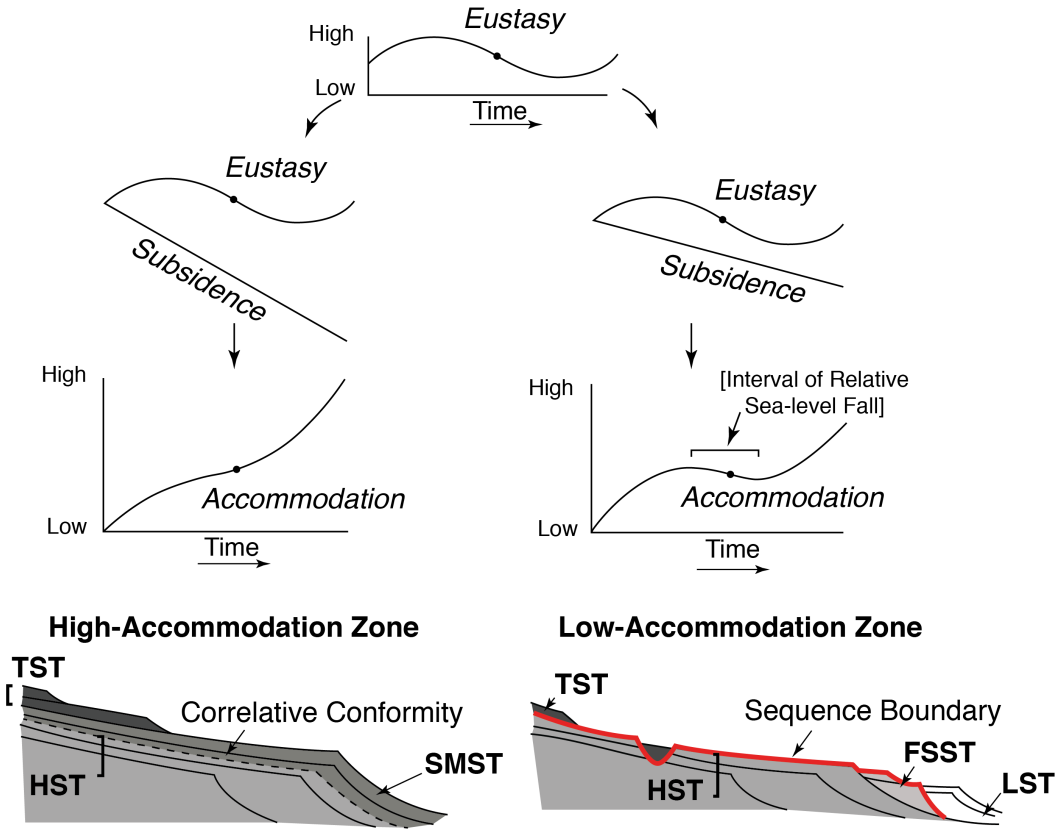
High
Low
Eustasy
Time
Eustasy
Subsidence
High
Low
Accommodation
Time
Eustasy
Subsidence
High
Low
[Interval of Relative
Sea-level Fall]
Accommodation
Time
High-Accommodation Zone
Low-Accommodation Zone
TST
Correlative Conformity
SMST
HST
TST
Sequence Boundary
FSST
HST
LST

Fig.5.— Stratal architecture for depositional sequences where a shoreline is in the high-accommodation zone (left) or low-accommodation zone (right). LST, lowstand systems tract; TST, transgressive systems tract; SMST, shelf-margin systems tract; HST, highstand systems tract; and FSST, falling-stage systems tract. Modified from Posamentier and Allen (1993).

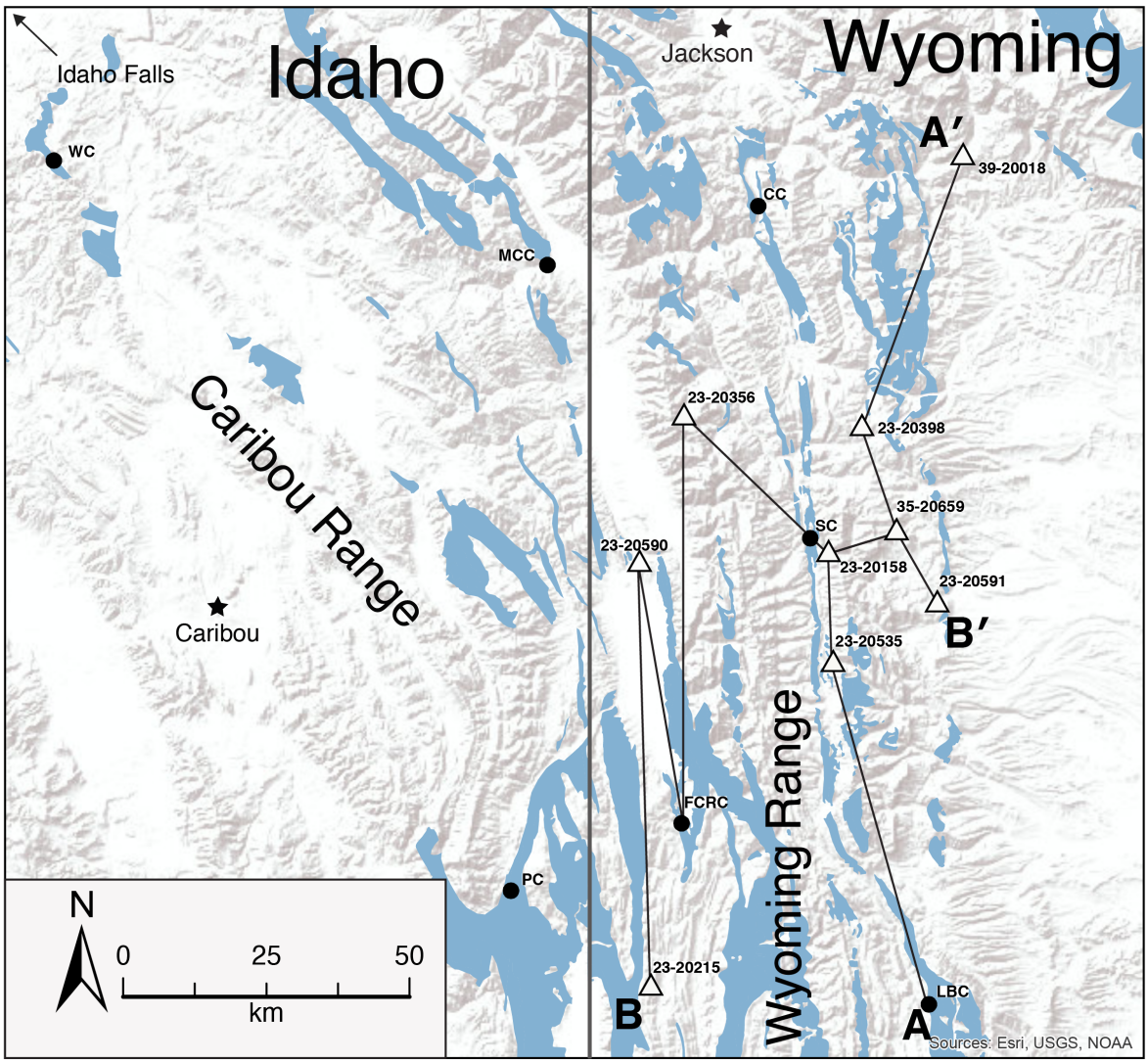
Idaho
Wyoming
Idaho Falls
Jackson
WC
MCC
CC
A′
39-20018
23-20356
23-20398
35-20659
SC
23-20590
23-20158
23-20591
B′
23-20535
Caribou Range
Caribou
Wyoming Range
FCRC
PC
23-20215
B
A
LBC
N
0
25
50
km
Sources: Esri, USGS, NOAA

Fig.6.— Jurassic outcrop (blue) in Wyoming and Idaho with lettered circles showing the location of the seven measured columns and numbered triangles showing the location of the nine well logs. Cross-sections A–A′ and B–B′ are indicated. CC, Cabin Creek; FCRC, Fish Creek Road Cut; LBC, La Barge Creek; MCC, McCoy Creek; PC, Preuss Creek; SC, Sheep Creek; WC, Wolverine Canyon.

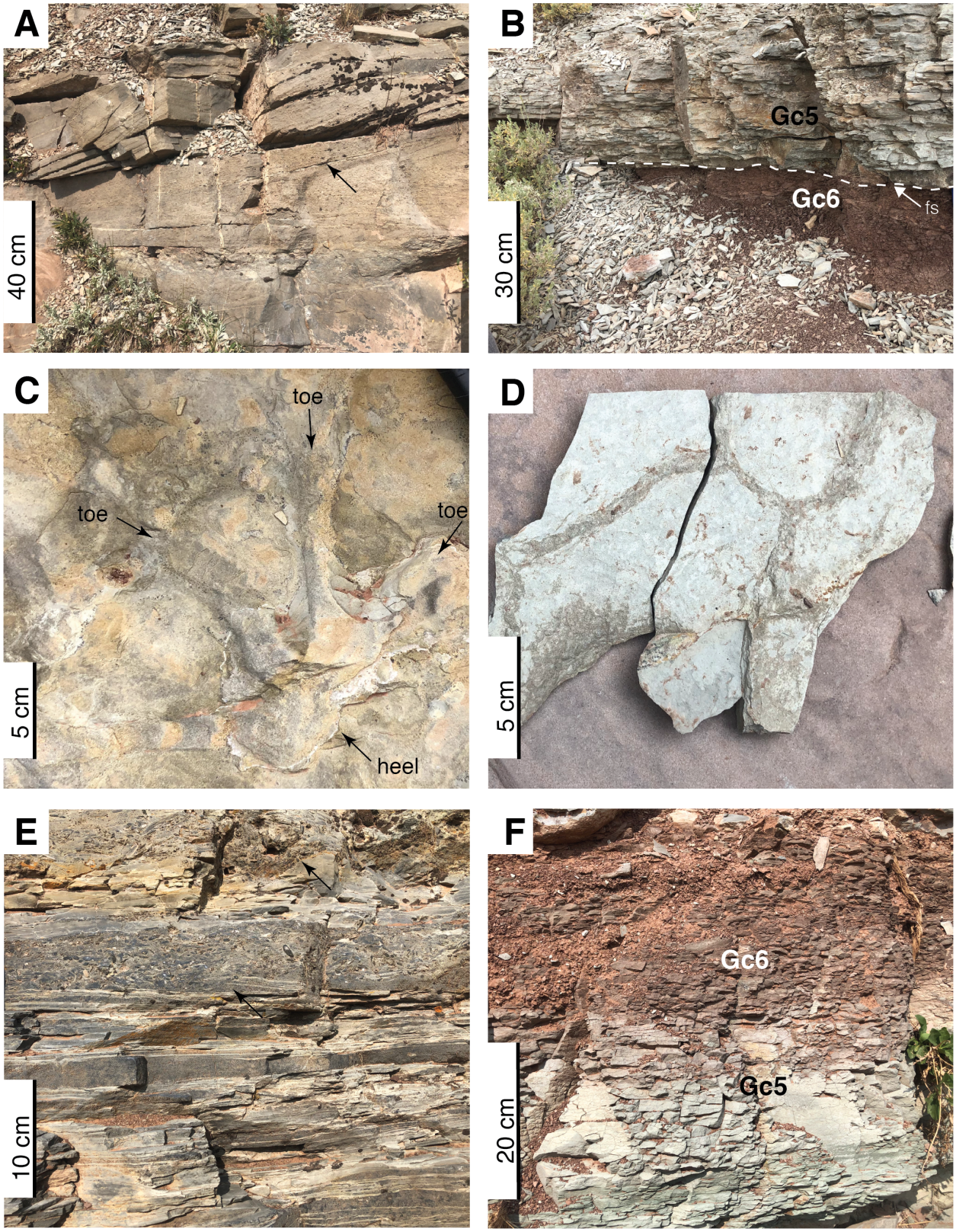
A
40 cm
B
Gc5
Gc6
fs
30 cm
C
toe
toe
toe
heel
5 cm
D
5 cm
E
10 cm
F
Gc6
Gc5
20 cm

Fig.7.— Outcrop photos of Facies Gc1, Gc2, Gc5, and Gc6. **A)** Photograph of Facies Gc2 at La Barge Creek showing large-scale trough cross stratification. Arrow points to shell lag at set boundary. **B)** Photograph of a flooding surface (fs) between Facies Gc6 and Gc5 at La Barge Creek. **C)** Photograph of a tridactyl dinosaur footprint in Facies Gc2 at La Barge Creek. Arrows point to three toes and heel. **D)** Photograph of desiccation cracks in Facies Gc6 at La Barge Creek. **E)** Photograph of a forced-regressive lag in Facies Gc1 at La Barge Creek. **F)** Photograph of Facies Gc5 grading upwards in to Facies Gc6 at La Barge Creek.

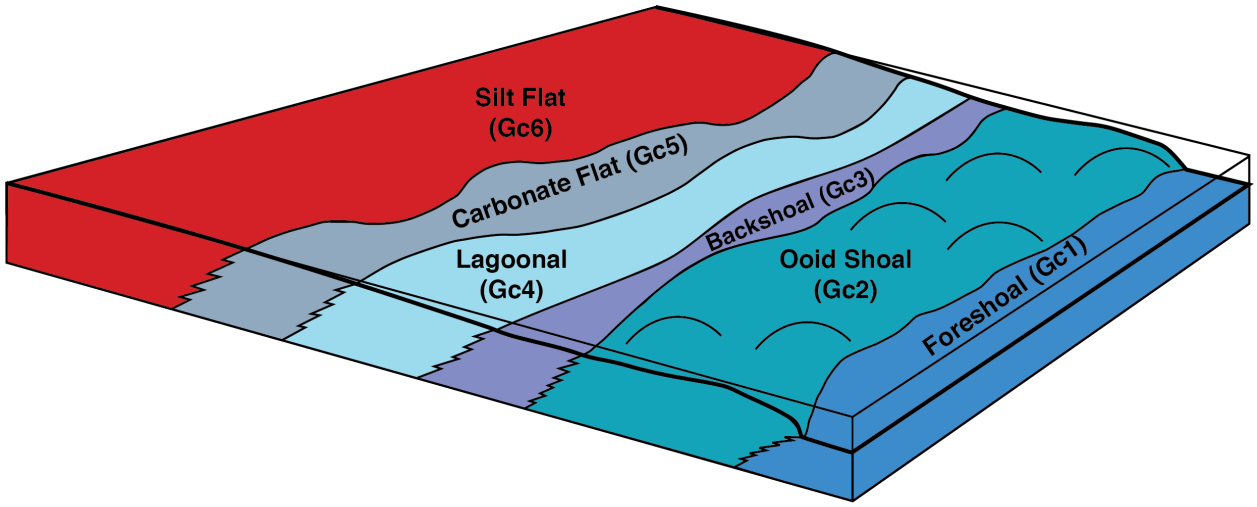
Silt Flat
(Gc6)
Carbonate Flat (Gc5)
Lagoonal
(Gc4)
Backshoal (Gc3)
Ooid Shoal
(Gc2)
Foreshoal (Gc1)

Fig.8.— Facies model showing the interpreted lateral relationships among facies in the Giraffe Creek Member of the Twin Creek Limestone. Gc1, Heterolithic Skeletal Ooid Grainstone; Gc2, Ooid Grainstone; Gc3, Heterolithic Carbonate Mudstone; GC4, Planar-laminated Lime Mudstone; Gc5, Dolomitic Lime Mudstone; Gc6, Red Siltstone.

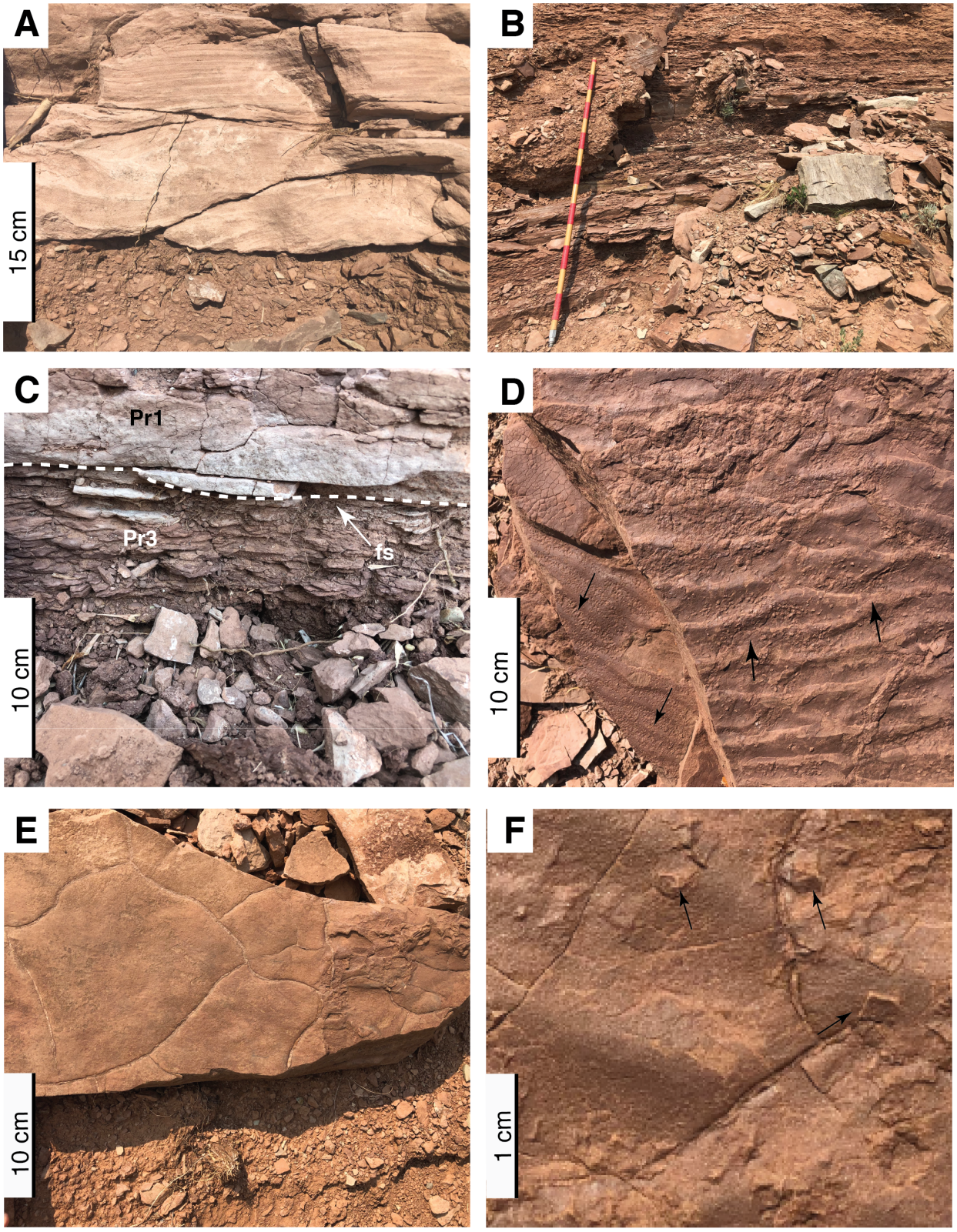
A
15 cm
B
C
Pr1
Pr3
ts
10 cm
D
10 cm
E
10 cm
F
1 cm

Fig.9.— Outcrop photos of Facies Pr1, Pr2, and Pr3. **A)** Photograph of Facies Pr1 at La Barge Creek showing large-scale trough cross stratification. **B)** Photograph of Facies Pr2 at La Barge Creek showing flaser and wavy bedding. Jacob staff marked in 10 cm increments. **C)** Photograph of Facies Pr3 at La Barge Creek showing a flooding surface (fs) between Facies Pr3 and Pr1. **D)** Photograph of 2D current ripples in Facies Pr2 at La Barge Creek. Arrows indicate direction of flow. **E)** Photograph of desiccation cracks in Facies Pr2 at La Barge Creek. **F)** Photograph of halite casts in Facies Pr2 La Barge Creek. Arrows point to halite casts.

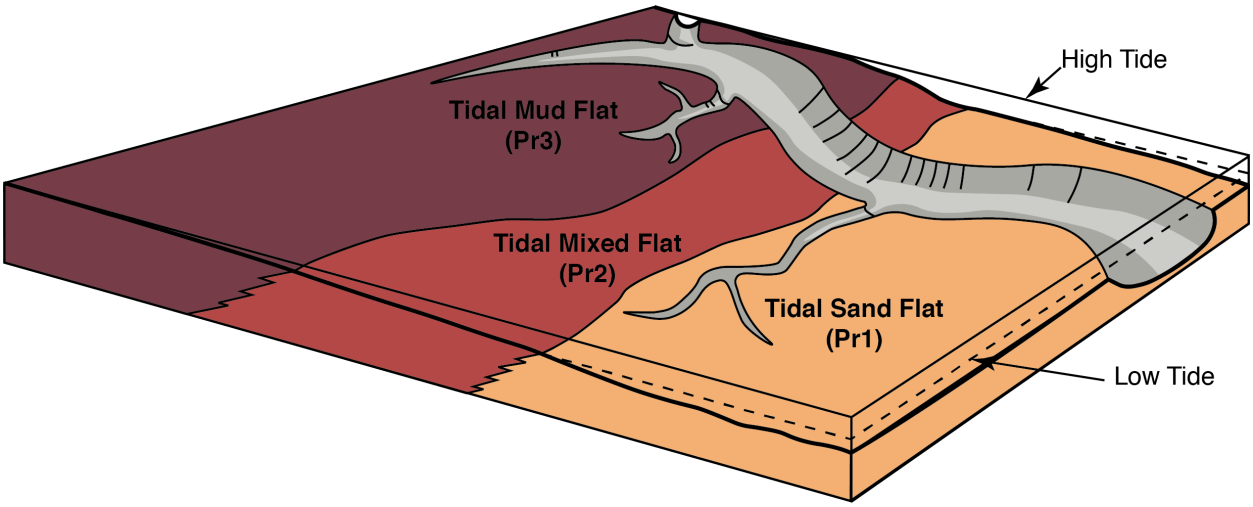
High Tide
Tidal Mud Flat
(Pr3)
Tidal Mixed Flat
(Pr2)
Tidal Sand Flat
(Pr1)
Low Tide

Fig.10.— Facies model showing the interpreted lateral relationships among facies in the Preuss Formation. Pr1, Cross-bedded Sandstone; Pr2, Heterolithic Silty Sandstone; Pr3, Red Mudstone.

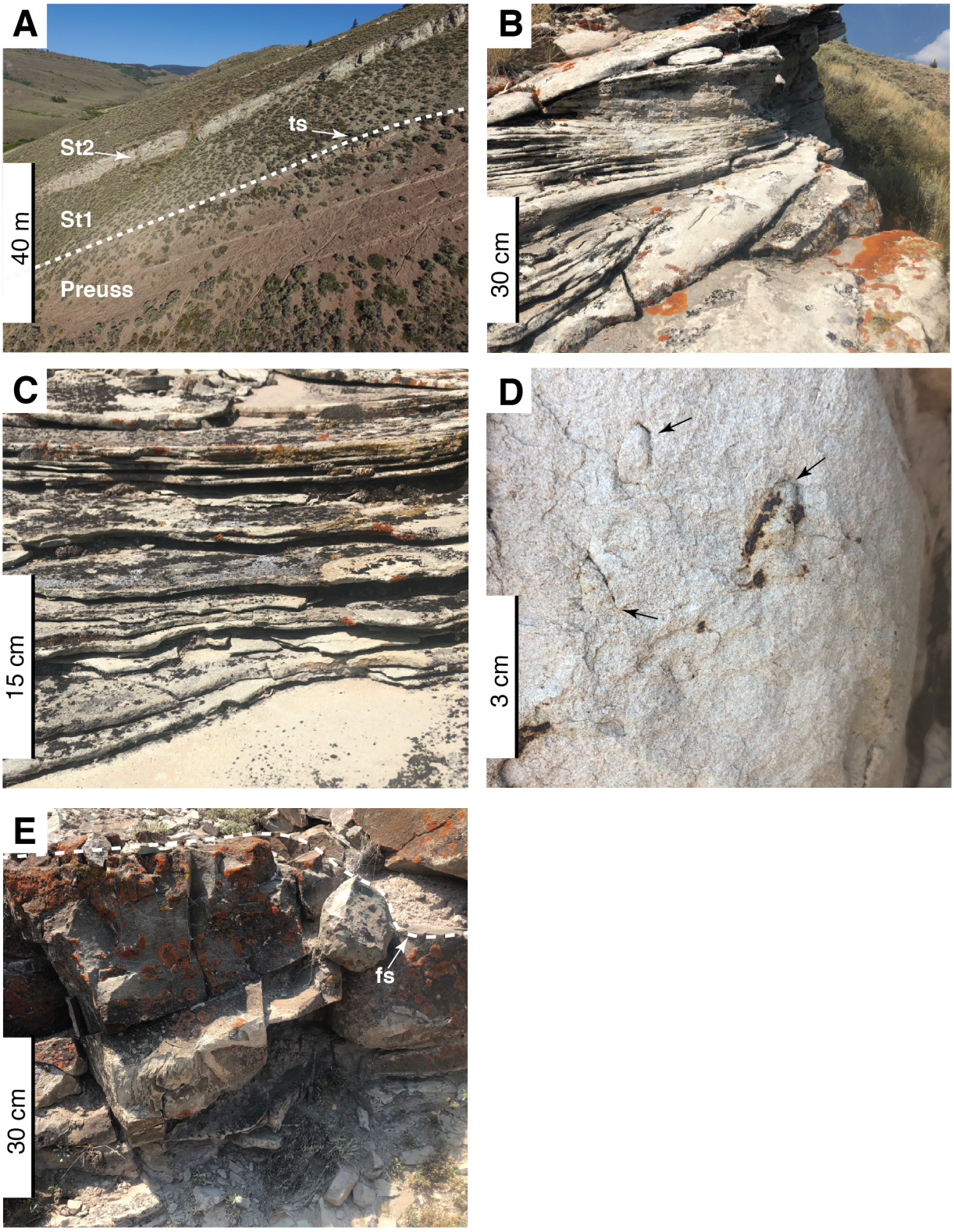
A
ts
St2
St1
Preuss
40 m
B
30 cm
C
15 cm
D
3 cm
E
fs
30 cm

Fig.11.— Outcrop photos of Facies St1, St2, St3. **A)** Aerial photograph of Facies St1 and St2 at La Barge Creek, with transgressive surface (ts). **B)** Photograph of large-scale cross stratification in Facies St2 at La Barge Creek. **C)** Photograph of planar laminae Facies St4 at La Barge Creek. **D)** Outcrop photograph of *Ophiomorpha* (arrows) in Facies St2 at La Barge Creek. **E)** Outcrop photograph of a mineralized flooding surface (fs) in Facies St3 at La Barge Creek.

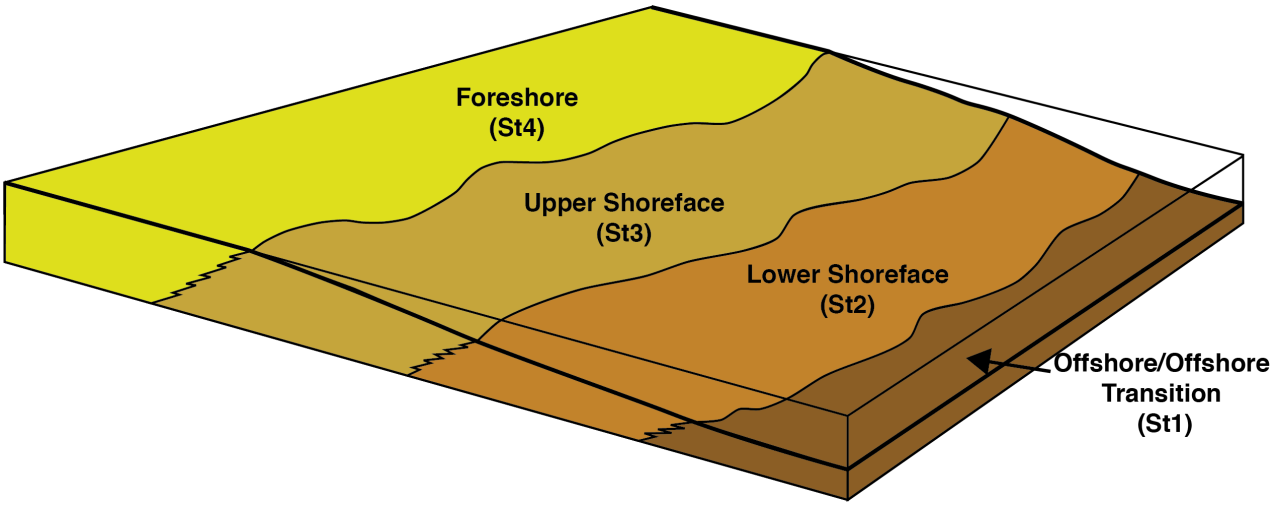
Foreshore
(St4)
Upper Shoreface
(St3)
Lower Shoreface
(St2)
Offshore/Offshore
Transition
(St1)

Fig.12.— Facies model showing the interpreted lateral relationships among facies in the Stump Formation. St1, Heterolithic Shale; St2, Amalgamated Sandstone; St3, Trough Cross-Stratified Sandstone; St4, Planar Laminated Sandstone.

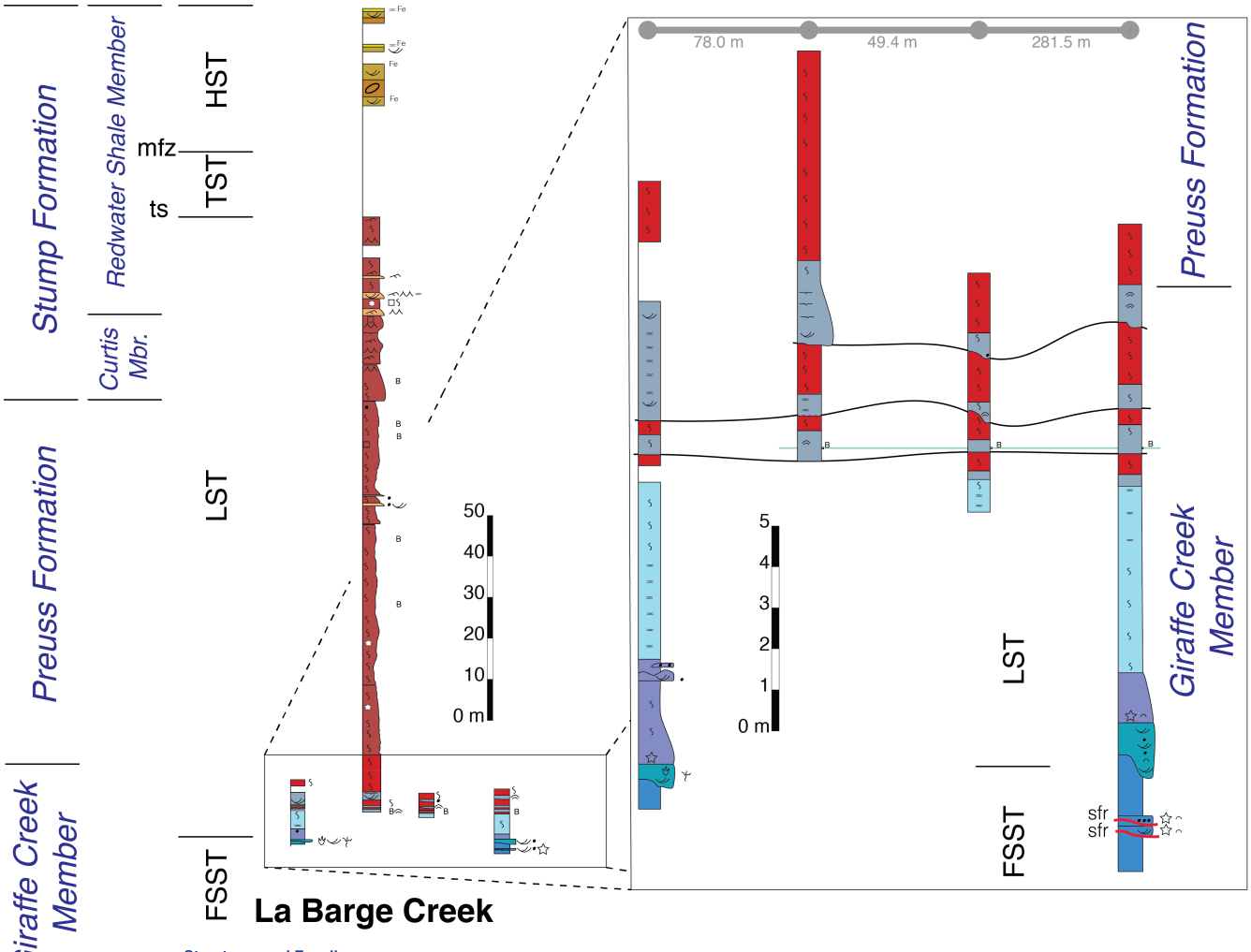

Structures and Fossils

- Gastropod
- Bivalve
- Trackway
- Ooid
- Ripple lamination
- Bioturbation
- Fe Iron staining
- Gypsum nodules
- Silicified anhydrite nodules
- Gypsum stringers
- Mosaic gypsum
- Dewatering structures
- B Bentonite
- *Ophiomorpha*
- Lithoclast
- Chert
- Syneresis cracks
- P Paleosol
- Vortex ripples
- Dessication cracks
- Crinoid
- Planar lamination
- Wavy lamination
- Thrombolitic microbial lamination
- Stromatolitic microbial lamination
- Trough cross stratification
- Halite casts
- *Thalassinoides*

Giraffe Creek member facies

- Gc7: Sabkha
- Gc6: Silt flat
- Gc5: Carbonate flat
- Gc4: Lagoonal
- Gc3: Backshoal
- Gc2: Ooid shoal
- Gc1: Foreshoal

Preuss Formation facies

- Pr5: Channel
- Pr4: Flood Plain
- Pr3: Mud Flat
- Pr2: Mixed Flat
- Pr1: Sand Flat
- Bentonite

Stump formation facies

- St4: Forshore
- St3: Upper shoreface
- St2: Lower shoreface
- St1: Offshore transition

Fig.13.— Stratigraphic column and sequence-stratigraphic interpretation of La Barge Creek. Detail of lateral variation in the Giraffe Creek–Preuss transition in shown in inset. ts, transgressive surface; mfz, maximum flooding zone; sfr, surface of forced regression; LST, lowstand systems tract; TST, transgressive systems tract; HST, highstand systems tract.

Stump
Preuss
Giraffe Creek
ts
180 m

Fig.14.— Panoramic photo of La Barge Creek, showing Giraffe Creek Member of the Twin Creek Formation, Preuss Formation, and Stump Formation. ts, transgressive surface.

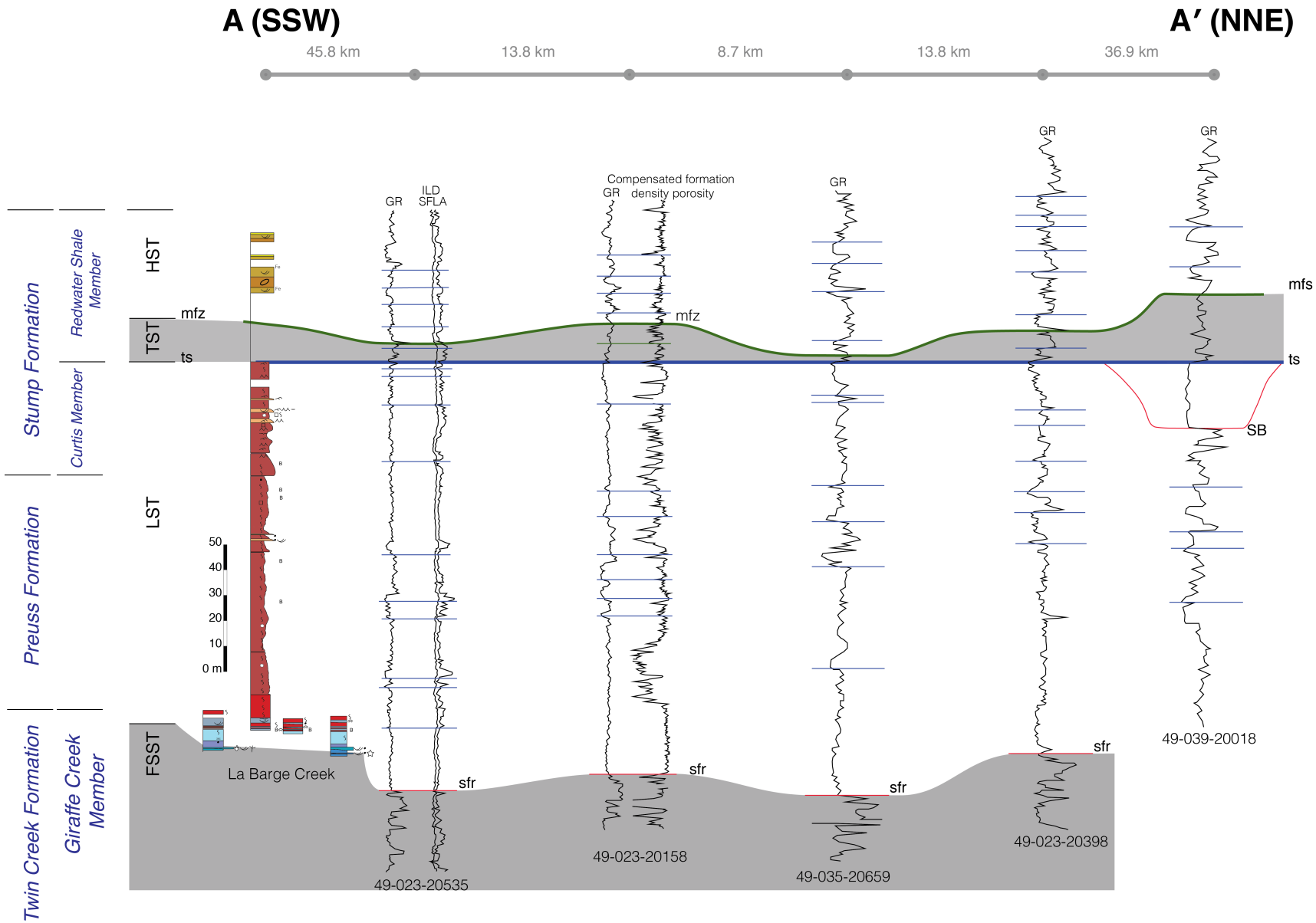
A (SSW)
A′ (NNE)
45.8 km
13.8 km
8.7 km
13.8 km
36.9 km
Twin Creek Formation
Giraffe Creek Member
Preuss Formation
Stump Formation
Curtis Member
Redwater Shale Member
FSST
LST
TST
HST
mfz
ts
mfs
sfr
SB
GR
ILD
SFLA
Compensated formation density porosity
La Barge Creek
50
40
30
20
10
0 m
49-023-20535
49-023-20158
49-035-20659
49-023-20398
49-039-20018

Fig.15.— Stratigraphic cross-section and sequence-stratigraphic interpretation of the measured section at La Barge Creek and five well logs along depositional dip cross-section line, A–A′ of Fig. 6. ts, transgressive surface; mfz, maximum flooding zone; sfr, surface of forced regression; LST, lowstand systems tract; TST, transgressive systems tract; HST, highstand systems tract. Flooding surfaces are indicated by blue lines. GR, gamma ray.

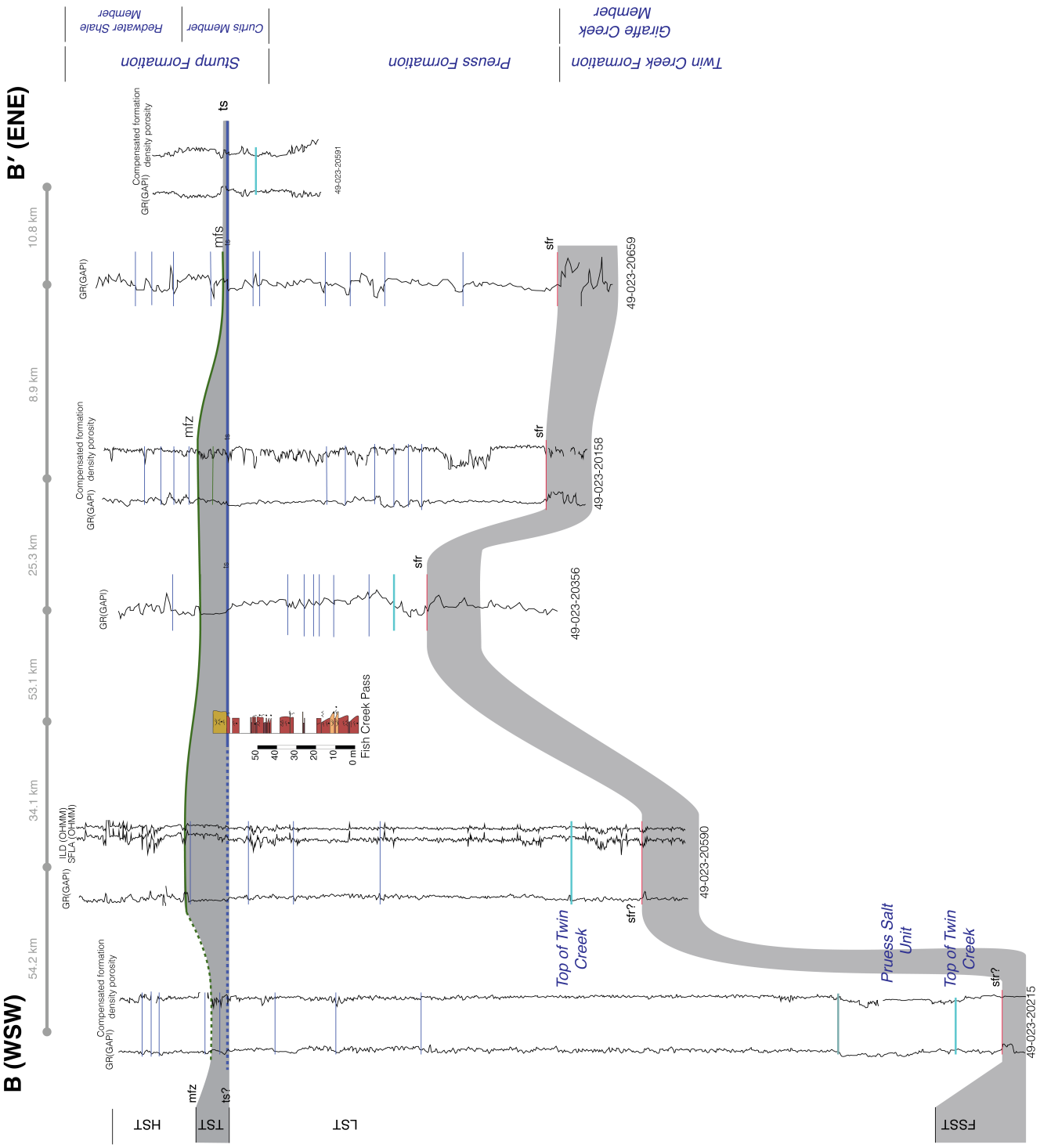
B (WSW)
B′ (ENE)
54.2 km
34.1 km
53.1 km
25.3 km
8.9 km
10.8 km
Stump Formation
Redwater Shale Member
Curtis Member
Preuss Formation
Twin Creek Formation
Giraffe Creek Member
HST
TST
LST
FSST
mfz
ts?
ts
mfs
sfr
sfr?
GR(GAPI)
ILD (OHMM)
SFLA (OHMM)
Compensated formation density porosity
Fish Creek Pass
50
40
30
20
10
0 m
49-023-20591
49-023-20659
49-023-20158
49-023-20356
49-023-20590
49-023-20215
Top of Twin Creek
Pruess Salt Unit
Top of Twin Creek

Fig.16.— Stratigraphic cross section and sequence-stratigraphic interpretation of the measured section at Fish Creek Road Cut and six well logs along an east west transect cross-section B–B′ of Fig. 6. ts, transgressive surface; mfz, maximum flooding zone; sfr, surface of forced regression; LST, lowstand systems tract; TST, transgressive systems tract; HST, highstand systems tract. Flooding surfaces are highlighted by dark blue lines. GR, gamma ray.

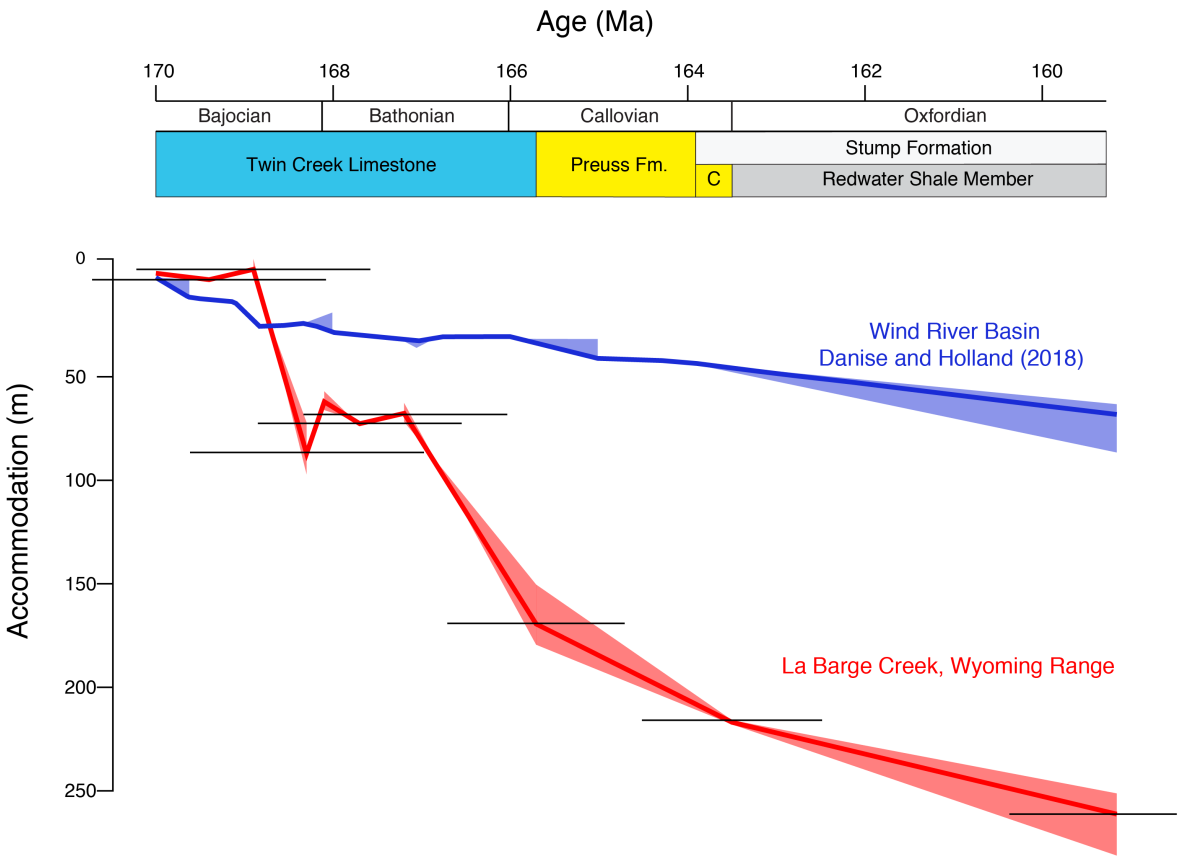
Age (Ma)
170
168
166
164
162
160
Bajocian
Bathonian
Callovian
Oxfordian
Twin Creek Limestone
Preuss Fm.
Stump Formation
C
Redwater Shale Member
Accommodation (m)
0
50
100
150
200
250
Wind River Basin
Danise and Holland (2018)
La Barge Creek, Wyoming Range

Fig.17.— Backstripped subsidence curves for the La Barge Creek stratigraphic column in southwestern Wyoming and a column from Danise and Holland (2018). Backstripping data based on the La Barge Creek column of this study and Howes (2017). Ages and their uncertainties based on the International Chronostratigraphic Chart (Cohen 2018). C, Curtis Member of the Stump Formation.

APPENDIX A: COORDINATES OF MEASURED SECTIONS AND WELL LOGS

Locality	Longitude	Latitude
Cabin Creek	-110.778	43.249
Fish Creek Road Cut	-110.898	42.540
La Barge Creek	-110.510	42.330
McCoy Creek	-111.110	43.182
Preuss Creek	-111.167	42.462
Sheep Creek	-110.697	42.868
Wolverine Canyon	-111.884	43.301

API Number	Longitude	Latitude
49-023-20535	-110.661	42.728
49-023-20158	-110.668	42.854
49-035-20659	-110.561	42.879
49-023-20398	-110.615	42.999
49-039-20018	-110.457	43.310
49-023-20215	-110.947	42.354
49-023-20590	-110.965	42.843
49-023-20356	-110.895	43.011
49-023-20591	-110.497	42.796

APPENDIX B: MEASURED COLUMNS

Structures and Fossils

- Gastropod
- Bivalve
- Trackway
- Ooid
- Ripple lamination
- Bioturbation
- Fe Iron staining
- Gypsum nodules
- Silicified anhydrite nodules
- Gypsum stringers
- Mosaic gypsum
- Dewatering structures
- B Bentonite
- *Ophiomorpha*
- Lithoclast
- Chert
- Syneresis cracks
- P Paleosol
- Vortex ripples
- Dessication cracks
- Crinoid
- Planar lamination
- Wavy lamination
- Thrombolitic microbial lamination
- Stromatolitic microbial lamination
- Trough cross stratification
- Halite casts
- *Thalassinoides*

Giraffe Creek member facies

- Gc7: Sabkha
- Gc6: Silt flat
- Gc5: Carbonate flat
- Gc4: Lagoonal
- Gc3: Backshoal
- Gc2: Ooid shoal
- Gc1: Foreshoal

Preuss Formation facies

- Pr5: Channel
- Pr4: Flood Plain
- Pr3: Mud Flat
- Pr2: Mixed Flat
- Pr1: Sand Flat

Stump formation facies

- St4: Forshore
- St3: Upper shoreface
- St2: Lower shoreface
- St1: Offshore transition

Cabin Creek
1 of 1

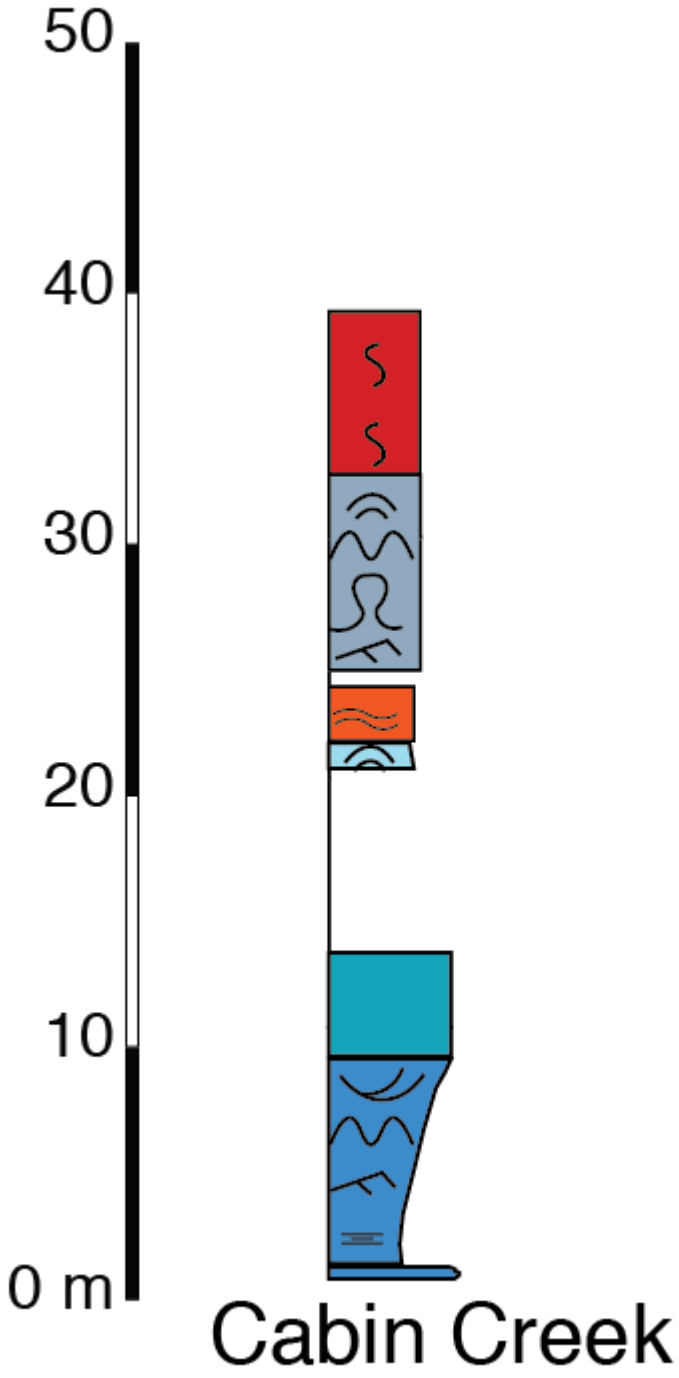

Fish Creek Pass
1 of 1

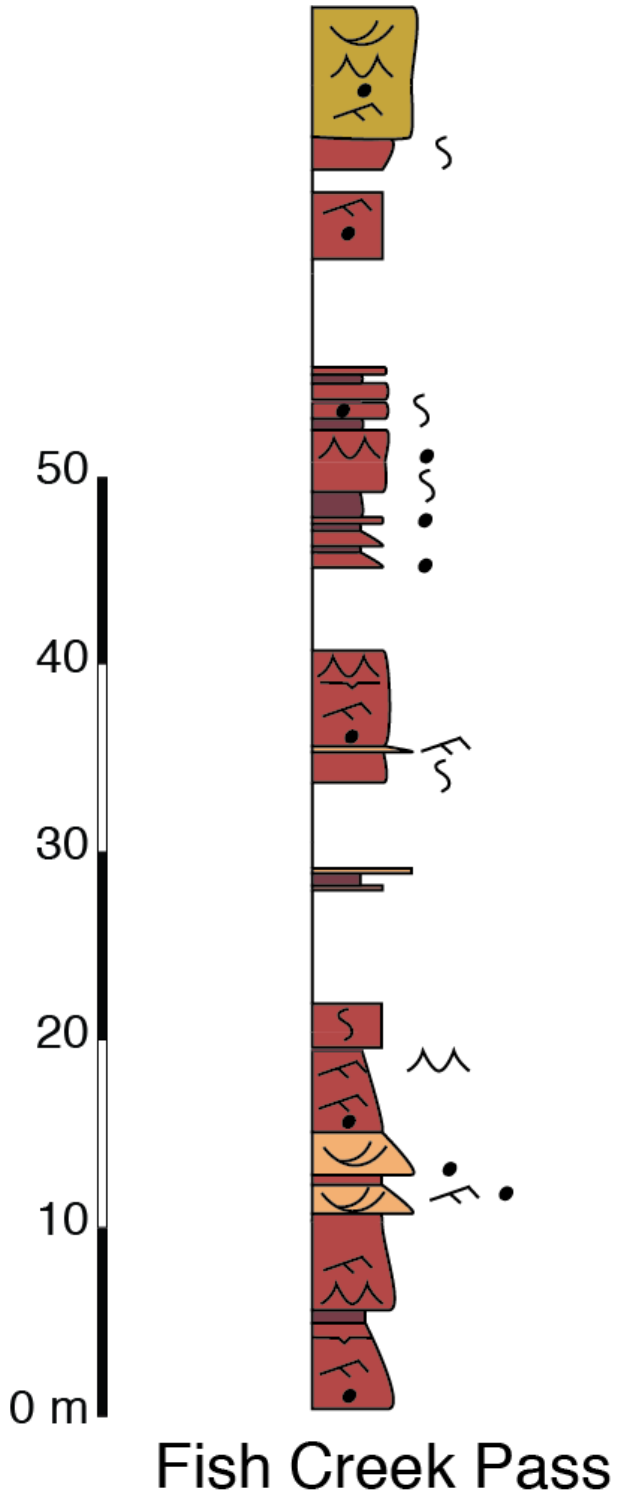

McCoy Creek
1 of 1

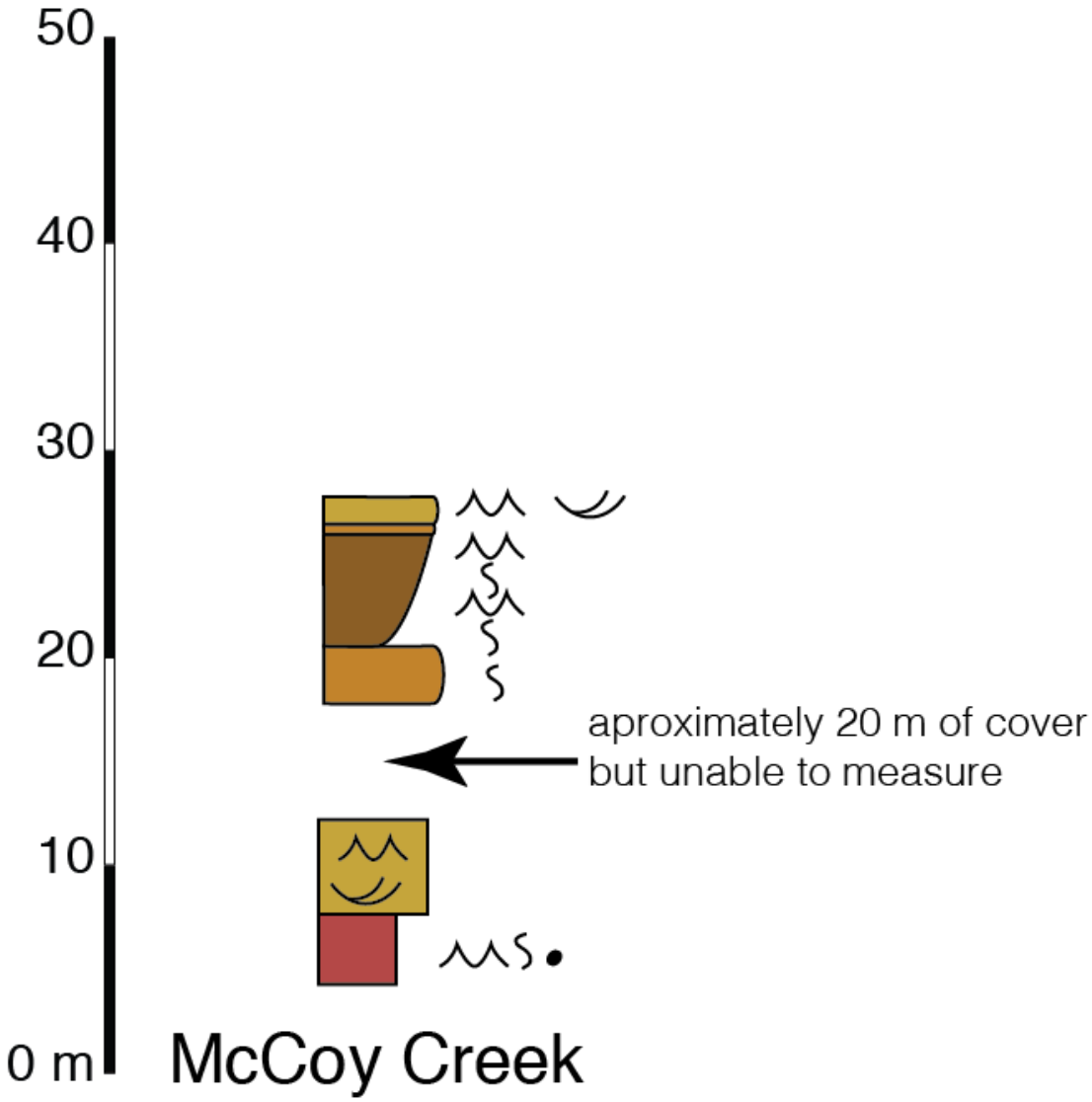

Preuss Creek
1 of 1

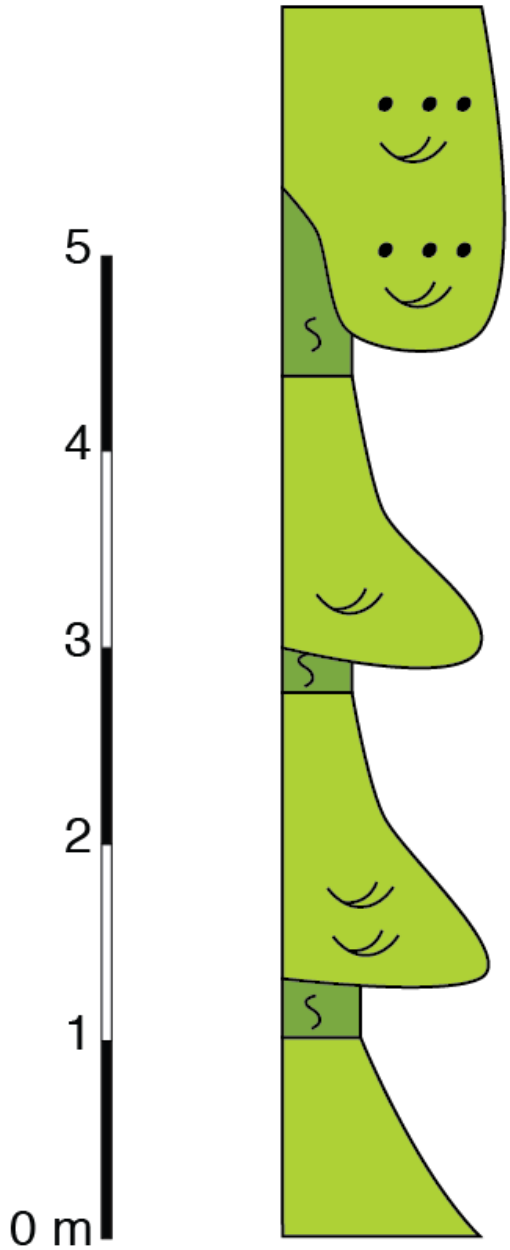

Preuss Creek

Sheep Creek
1 of 1

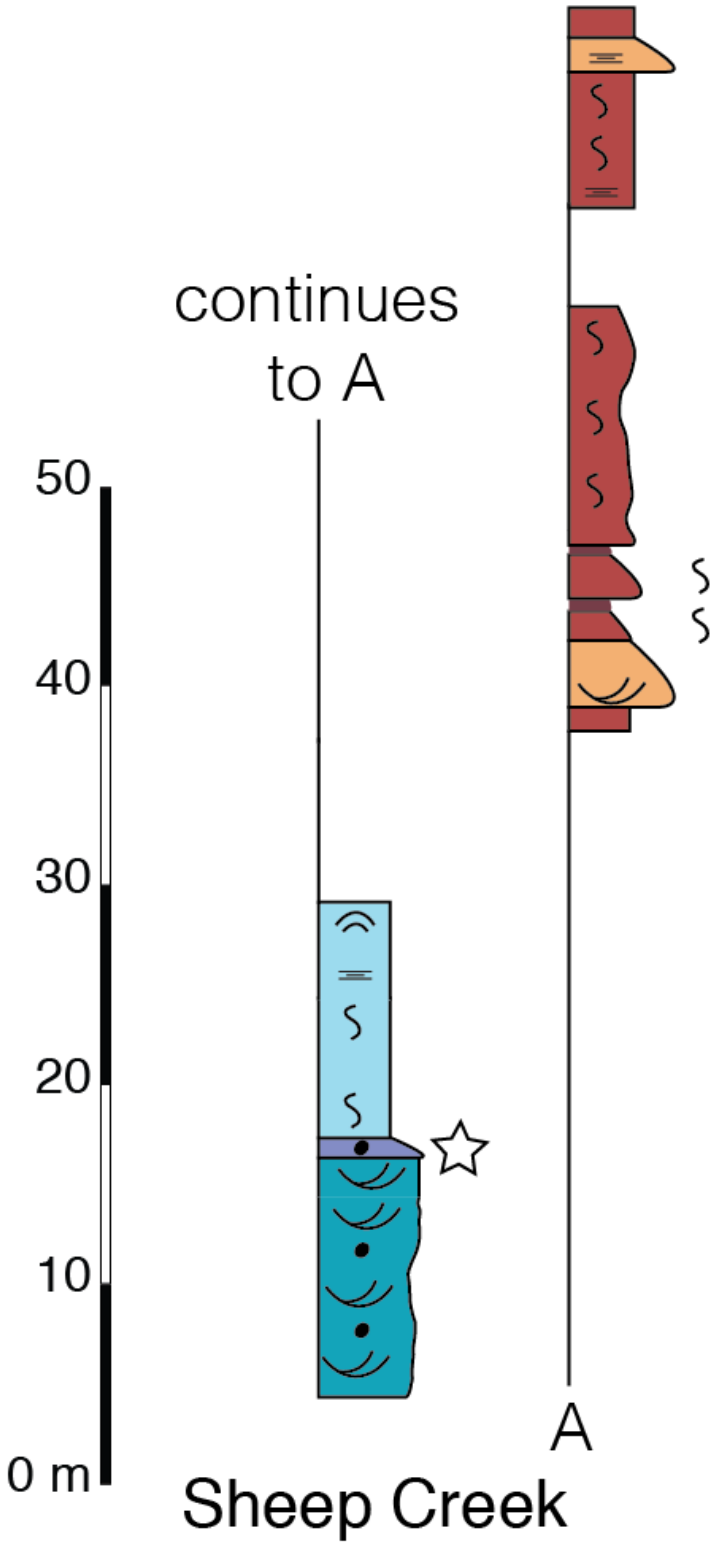

Wolverine Canyon
1 of 3

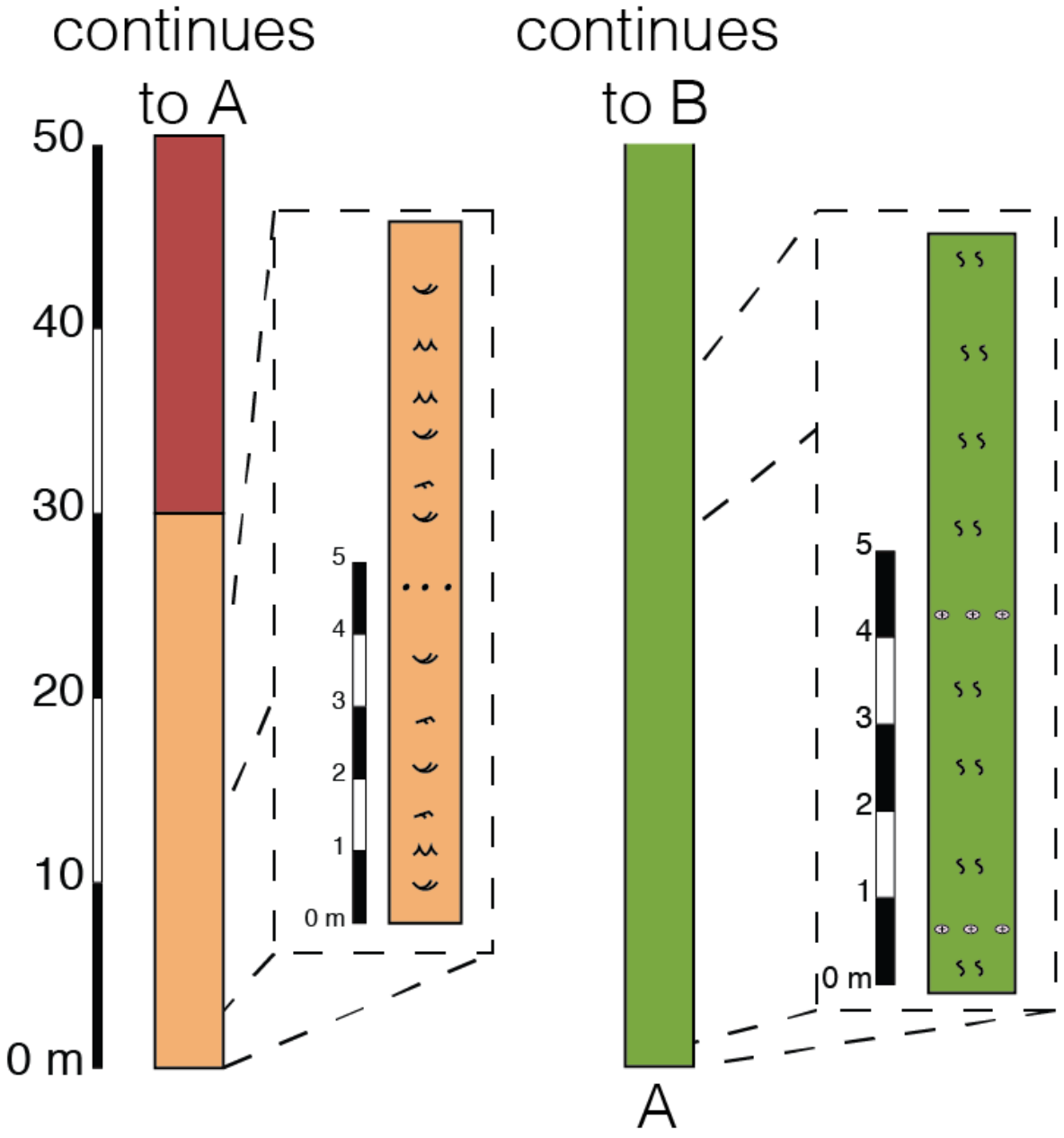

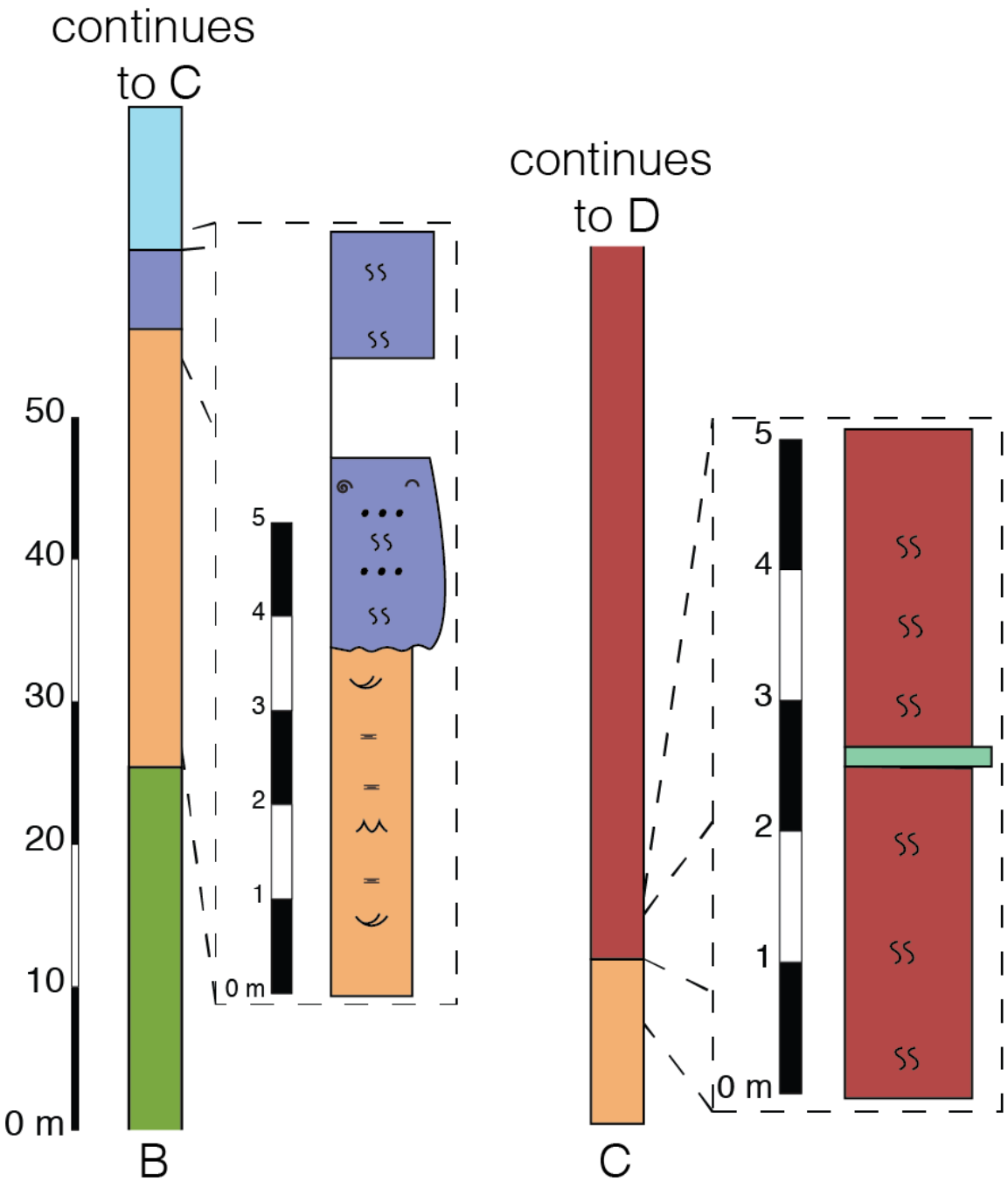
continues
to C
50
40
30
20
10
0 m
B
5
4
3
2
1
0 m
continues
to D
C
5
4
3
2
1
0 m

Wolverine Canyon
3 of 3